Terthienyl carbene complexes

by

Mmushi Moses Moeng

Submitted in partial fulfillment for the degree

MAGISTER SCIENTIA

in

CHEMISTRY

in the Faculty of Natural & Agricultural Science

UNIVERSITY OF PRETORIA
PRETORIA

Supervisor: Professor Simon Lotz

March 2001

Acknowledgments

I wish to express my sincere gratitude and appreciation to the following:
The creator for His guidance and the ability and perseverance granted to me to complete my studies;
My supervisor, Prof. Simon Lotz, for his guidance, encouragement and insight;
Mr Eric Palmer for recording of NMR spectra;
Dr Helmar Görls for structural elucidations of crystallographic data;
Dr.M.Landman and Dr.T.A.Logothetis for their individual roles in completion of this study;
My mother Priscilla Moeng, aunt Accamia and family for their support and understanding;
All my fellow Organometallics students and friends;
The National Research Foundation for financial support.

Thank you
Moses

Summary

Terthienyl (HTTTH) forms part of the family of conjugated 5-membered heterocycles and although many novel conversions of thiophenes and their derivatives have been recorded, the coordination chemistry of terthienyl has been neglected.

Dinuclear biscarbene complexes $[(CO)_5MC(OEt)TTTC(OEt)M(CO)_5]$, and monocarbene complexes $[M(CO)_5\{C(OEt)TTTH\}]$ of the transition metals Cr, Mo and W with terthienyl spacer units were prepared. The reactivity of these complexes with ammonia, their relative stability and their structural features were investigated. The study focuses on electron delocalization of the conjugated TTT moiety and the role of the TTT substituent in stabilizing the electrophilic carbene carbon.

Terthienyl substrates are readily mono and dimetallated and the classical Fischer method for the synthesis of carbene complexes was used. Complexes were fully characterized and molecular structures were determined. A single crystal structure determination of the tungsten biscarbene complex indicated a planar configuration of the thienyl rings and partial delocalization through the conjugated ring system.

Samevatting

Tertiëniel (HTTTH) het 'n gekonjugeerde 5-lid heteroatoomring en behoort tot die familie van aromatiese heteroatoomverbindings. Alhoewel baie nuwe omskakelings van tiofeen en hulle derivate in die literatuur beskryf is, is die koördinasiechemie van tertiëniel nog min bestudeer.

In hierdie studie, is bimetaal biskarbeenkomplekse, $[(CO)_5MC(OEt)TTTC(OEt)M(CO)_5]$, en monokarbeenkomplekse $[M(CO)_5\{C(OEt)TTTH\}]$ van die oorgangsmetale Cr, Mo en W met tiëniel spasieërders berei. Die reaktiwiteit van hierdie nuwe komplekse teenoor ammoniak, hul relatiewe stabiliteite en hul struktuureienskappe is ondersoek. Die studie fokus verder op elektrondelokalisasie van die konjugeerde TTT skakel en die rol van die TTT fragment as 'n substituent in die stabilisering van die elektrofiliese karbeenkoolstof atoom.

Tertiëniel substrate word geredelik mono- en digemetalleer en die klassieke Fischer-metode is gebruik vir die sintese van die karbeenkomplekse. Die komplekse is volledig gekarakteriseer en molekulêre strukture is bepaal. Die kristalstruktuurbepaling van die wolfram biskarbeenkompleks dui op 'n planêre konformasie vir die tiënielringe en 'n gedeeltelike delokalisering deur die gekonjugeerde ringsisteem.

CONTENTS

List of abbreviations

PA	:	Polyacetylene
PTs	:	Polythiophenes
CPs	:	Conducting polymers
HTTTH	:	α-Terthienyl
M	:	Transition metal
M-C	:	Metal-carbon linkage
HDS	:	Heterogeneous hydrodesulfurization
DMF	:	Dimethylformamide
LiTTTLi	:	Dilithiated terthienyl
THF	:	Tetrahydrofuran
BuLi	:	Butyllithium
TMEDA	:	Tetramethyl ethylene diamine
NMR	:	Nuclear magnetic resonance
ppm	:	Parts per million
δ	:	Chemical shift
2D HETCOR	:	Two dimensional HETeronuclear CORrelation
COSY	:	COrrelated SpectroscopY
M^+	:	Molecular ion
UV	:	Ultraviolet
q	:	Quartet
s	:	Singlet
t	:	Triplet
d	:	Doublet
dd	:	Doublet of doublets
DTPH	:	3-Dimethylamino-1-(2-thienyl)-propanone·HCl
DTB	:	1,4-Di-(2-thienyl)-1,4-butanedione
DAH	:	Dimethylamine·HCl
Mb	:	Mannich base
MbH	:	Mannich base.HCl

List of compounds

1:

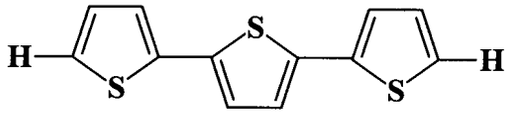

2:

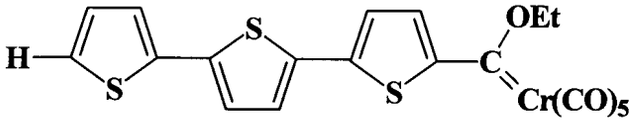

3:

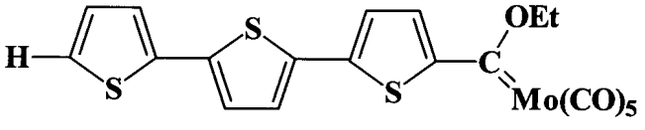

4:

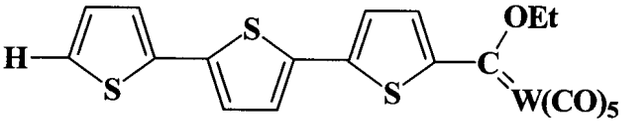

5:

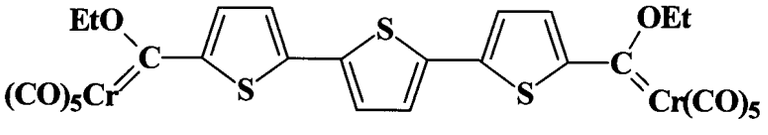

6:

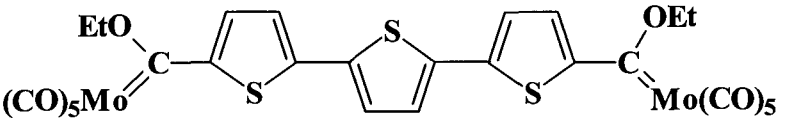
EtO
C
(CO)5Mo
S
S
S
OEt
C
Mo(CO)5

7:

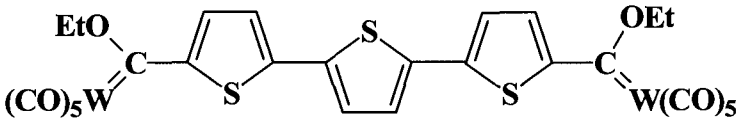
EtO
C
(CO)5W
S
S
S
OEt
C
W(CO)5

8:

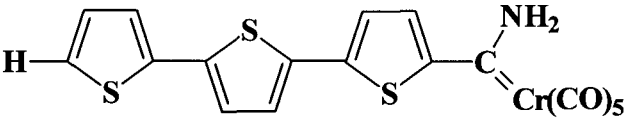
H
S
S
S
NH2
C
Cr(CO)5

9:

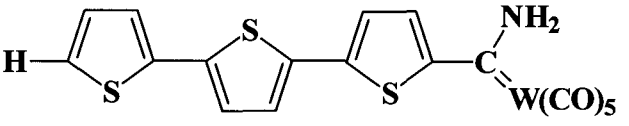
H
S
S
S
NH2
C
W(CO)5

10:

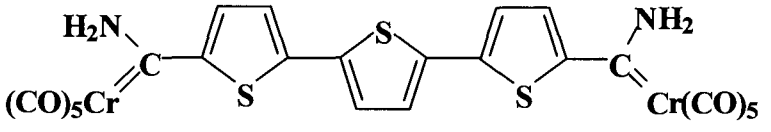
H2N
C
(CO)5Cr
S
S
S
NH2
C
Cr(CO)5

11:

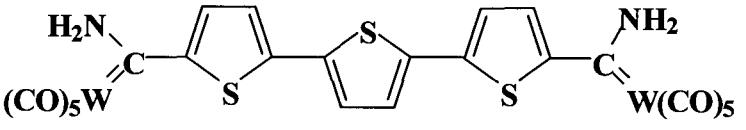
H2N
C
(CO)5W
S
S
S
NH2
C
W(CO)5

CHAPTER 1

INTRODUCTION

The current industrial approach is driven by productivity hence, new materials with great processability are required. Scaling down of the electronic circuits using new technologies like nanolithography have had only a marginal industrial appeal[1]. In the recent past, there has been much interest in the synthesis of future potential molecular wires, liquid crystals, optical materials and precursors for organic syntheses[2].

Dinuclear complexes containing bridges composed of different organic units have been reported[1]. There is a huge number of variations in the bridge composition that can be imagined, but our energy will be focused on terthienyl bridged complexes. Carbene complexes of poly(acetylene)[1] and thiophene,[3] to name few, have already been prepared. Thiophene has a pseudoaromatic character and displays diverse coordinating abilities towards transition metals[4].

Recently, in the year 2000, three scientists, Heeger, MacDiamid and Shirakawa, won the 2000 Nobel prize in chemistry for their fundamental research on the enhanced conductivity of activated polyacetylene.

---

1 F.Paul, C.Lapinte, Coord.Chem.Rev., 1998, 178-180, 431.

2 (a) M.H.Chisholm, Angew.Chem.Int.Ed.Engl., 1991, 30, 673.

(b) H.S.Nalwa, Appl.Organomet.Chem.,1991, 5, 349.

(c) Y.Zhou, J.W.Seyler, W.Weng, A.M.Arif, J.A.Gladysz, J.Am.Chem.Soc., 1993, 115, 8509.

3 (a) M.Landman, H.Görls, S.Lotz, J.Organomet.Chem., 2001, 285, 617.

(b) Y.M.Terblans, S.Lotz, J.Chem.Soc., Dalton Trans., 1997, 2177.

(c) M.Landman, H.Görls, S.Lotz, Eur.J.Inorg.Chem., 2001, 233.

(d) Y.M.Terblans, H.M.Roos, S.Lotz, J.Organomet.Chem., 1998, 566, 133.

4 R.Angelici, Coord.Chem.Rev., 1990, 105, 61.

They found that a thin film of polyacetylene could be oxidized with iodine vapour, thus increasing its conductivity a billion times. In the light of this year's Nobel prize in chemistry, there lies a bright future ahead for electronic components based on conducting polymers and polymer-based intergrated circuits. Soon, these components will find their place in the consumer products where low processing costs could become more important than high speed.

There are some conductive polymers that have come onto the market recently and are undergoing trials for potential applications. Polythiophene derivatives are of great commercial use in antistatic[2] treatment of photographic films, as sophisticated molecular devices in organic electronic compounds or selective modified electrodes and sensors[5]. They can also be used in devices in supermarkets for marking products[6]. This chapter gives a brief introduction about the versatility of the bridging ligands, dinuclear carbene complexes and the concepts of bonding in carbene complexes.

1.1 CONJUGATED BRIDGING LIGANDS

In organometallic polymers, unsaturated hydrocarbons act as electronic bridges[7] between two metals. Preparation of $(CH)_x$ complexes in the form of shiny coherent films stimulated an interest in the field of conducting polymers as a new class of electronic materials.

1.1.1 Polyethylenes

Figure 1.1 Polyolefins

[5] J.Roncali, Chem.Rev.,1992, 92, 711.

[6] www.nobel.se/announcement/2000/cheminfoen.htm or www.kva.se.

[7] J.Li, A.D.Hunter, R.McDonald, B.D.Santasiero, S.G.Bott, J.L.Atwood, Organometallics, 1992, 11, 3050.

Polyacetylene (PA), which is the simplest conjugated conducting polymer, consists of weakly coupled chains of CH units forming a pseudo-one-dimensional lattice. Both *trans* and *cis* forms can be prepared, but the *trans* isomer is thermodynamically more stable.

1.1.2 Polythiophenes

It has been reported that doping of PA in charge transfer reactions with an oxidizing or reducing agent could enhance the conductivity of the polymer dramatically[8].

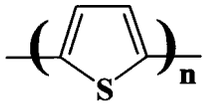

Figure 1.2 Polythiophenes

Polythiophenes (PTs) have rapidly become the topic of considerable interest. They have often been considered as models for the study of charge transport in conducting polymers (CPs) and their structural versatility has led to novel developments aimed at applications such as conductor electrode materials and organic conductors[6]. They are flat planar molecules and display π-delocalization.

[8] (a) H.Shirakawa, E.J.Louis, A.G.McDiarmid, C.K.Chiang, A.J.Heeger, J.Chem. Soc., Chem.Commun., 1978, 578.

(b) C.K.Chiang, C.R.Fincher, Y.W.Park, A.J.Heeger, H.Shirakawa, E.J.Louis, S.C.Gau, A.G.McDiarmid, Phys.Rev.Lett., 1977, 39, 1098.

PTs have been studied intensely with regard to their multiple technological applications such as antistatic coatings to sophisticated molecular devices[2,9]. PTs and derivatives are stable compounds and one of the most important aspect of these heterocycles is the ease of 2-substitution, which can be used to prepare new polymers with exciting properties.

The essential structural feature of PTs is the conjugated π-system extending over a large number of recurrent monomeric units. The characteristic feature of these complexes results in low dimensional materials with a high anisotropy of conductivity which is higher along the chain direction. PTs can be viewed as sp^2 carbon chains which are structurally similar to that of *trans*$(CH)_x$ connected units which is stabilized by the sulfur. This is illustrated in figure 1.3.

Figure 1.3 Structural comparison of *trans*$(CH)_x$ units and PT's

PTs have been the topic of many reviews since the inception of conjugated polyheterocycles in 1979[10]. However, until now, the only review specifically focused on PTs was published in 1986 and covered the early developments of the field upto 1985[11]. PTs are easily synthesized and various methods have been published outlining the synthesis. They are essentially prepared by means of two main routes, i.e. the chemical and the electrochemical syntheses[2].

---

9 K.R.J.Thomas, J.T.Lin, Yu S.Wen, Organometallics, 2000, 19, 1008.

10 A.F.Diaz, K.K.Kanazawa, G.P.Gardini, J.Chem.Soc.,Chem.Commun., 1979, 635.

11 G.Tourilon, Handbook of Conducting Polymers, Skotheim,T.A., Ed., Marcel Decker: New York, 1986, 294.

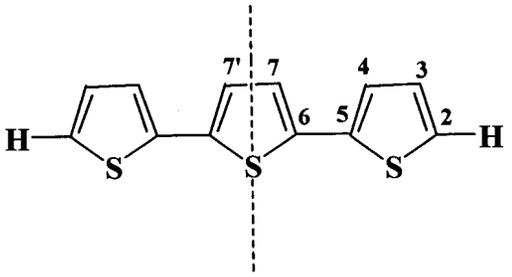

Figure 1.4 Atom numbering of terthienyl

Of particular interest in this study is terthienyl ($C_{12}H_8S_3$) in figure 1.4. Synthesis of terthienyl (HTTTH) was based on Stetter's work in which an aldehyde undergoes a Michael addition to an α-unsaturated ketone (Mannich base) in the presence of a cyanide as catalyst, affording 1,4-diketone[(1,4-di(2-thienyl)-1,4-butanedione]. Cyclization by P_2S_5/sodium carbonate gave terthienyl[12].

1.2 DINUCLEAR TRANSITION METAL COMPLEXES WITH A CONJUGATE LIGAND SYSTEM

Electron transfer and photoinduced energy processes in molecular devices are the basic steps in charge separation devices, light harvesting systems or in certain sensors and switches[13]. A wide range of dinuclear transition metal complexes with σ- or π-bonded hydrocarbon bridges/spacers have been synthesized[14] and sufficient information about these complexes and their syntheses is available, hence closer investigation into their reactivity and their potential applications in materials are important for further research.

---

12 H.Wynberg, J.Metselaar, Synth.Commun., 1984, 14, 1.

13 (a) F.Scandola, M.T.Indelli, C.Chiorboli, C.A.Bignozzi, Top.Curr.Chem., 1990, 158, 73.

(b) J.-P.Sauvage, J.-P.Collin, J.C.Chambron, S.Guillerez, C.Coudret, V.Balzani, F.Barigelletti, L.De Cola, L.Flamigni, Chem.Rev., 1994, 94, 993.

(c) V.Balzani, A.Juris, M.Venturi, S.Campagna, S.Serroni, Chem.Rev., 1996, 96, 759.

(e) G.Denti, S.Campagna, S. Serroni, M.Ciano, V.Balzani, J.Am.Chem.Soc., 1992, 114, 2944.

(f) S.Serroni, G.Denti, A.Juris, M.Ciano, V.Balzani, Angew.Chem.Int.Ed.Engl., 1992, 31, 1495.

(g) A.Juris, V.Balzani, F.Barigelleti, S.Campagna, P.Belser, A.von Zelewsky, Coord.Chem.Rev., 1988, 84, 85.

14 W.Beck, B.Niemer, M.Weiser, Angew.Chem.Int.Ed.Engl., (1993), 21, 923.

Metal complexes with conjugated hydrocarbon or carbon bridges (double bonds and triple bonds) and with donor or acceptor ligands as depicted in figure 1.5 are candidates for electrically conducting materials and for materials with second and third order non-linear optical properties[5,15]. These complexes can conduct only if charge can be delocalized along the entire polymer backbone, including the organic spacer, attaching atoms and metal fragments.

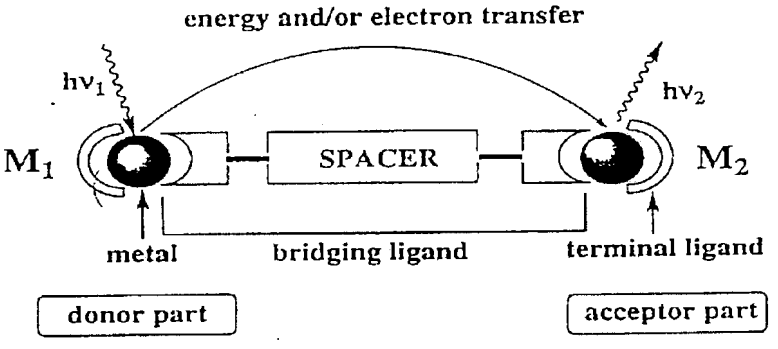

Figure 1.5 Schematic representation of the construction of photoactivated dinuclear metal complex

[15] (a) I.R.Whittal, M.G.Humphrey, S.Houbrechts, J.Maes, A.Persoons, S.Schmid, D.C.R.Hockless, J.Organomet.Chem., 1997, 544, 277.

(b) I.R.Whittal, M.P.Cifuentes, M.G.Humphrey, B.Lutherdavies, M.Samoc, S.Houbrechts, A.Persoons, G.A.Heath, D.C.R.Hockless, J.Organomet.Chem., 1997, 549, 127.

(c) A.M.McDonagh, I.R.Whittal, M.G.Humphrey, D.C.R.Hockless, B.W.Skelton, A.H.White, J.Organomet.Chem., 1996, 523, 33.

(d) A.M.McDonagh, M.P.Cifuentes, I.R.Whittal, M.G.Humphrey, M.Samoc, B.Lutherdavies, D.C.R.Hockless, J.Organomet.Chem., 1996, 526, 99.

Binuclear complexes of types A, B, C and D with various lengths of the carbon chain C_x ($x \leq 20$)[16] have been prepared[17] and display a rod-like appearance. They are shown in figure 1.6.

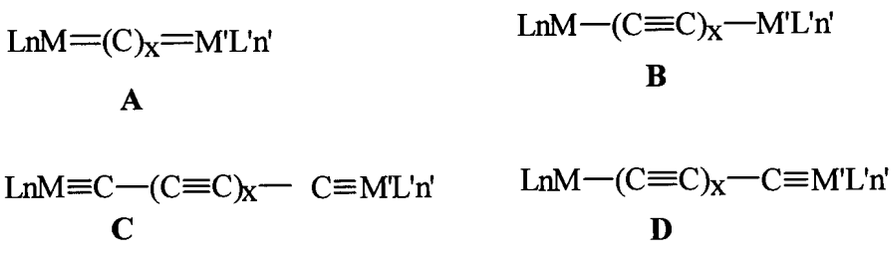

Figure 1.6 Dinuclear complexes with linear conjugated spacers

The dinuclear complexes with nonlinear conjugated spacers (A to E) in figure 1.7 have also been isolated and some of them have found application[1,18]. These spacers show branching and the metals are not directly opposite one another.

Until now complexes of this type have been rarely studied especially when it comes to application as molecular wires[19], liquid crystals and as precursors for heterometallic catalysis[17,20].

---

[16] (a) H.Lang, Angew.Chem.Int.Ed.Engl., 1994, 33, 547.
(b) U.H.F.Bunz, Angew.Chem.Int.Ed.Engl., 1996, 35, 969.
(c) T.Bartik, W.Weng, J.A.Ramsden, S.Szafert, S.B.Faloon, A.M.Arif, J.A.Gladysz, J.Am.Chem.Soc., 1998, 120, 11071.

[17] T.Bartik, B.Bartik, M.Brady, R.Dembinski, J.A.Gladysz, Angew.Chem.Int.Ed.Engl., 1996, 35, 414.

[18] F.Coat, M.-A.Guillevic, L.Toupet, F.Paul, C.Lapinte, Organometallics, 1997, 16, 5988.

[19] W.A.Hermann, Angew.Chem.Int.Ed.Engl., 1982, 21, 117.

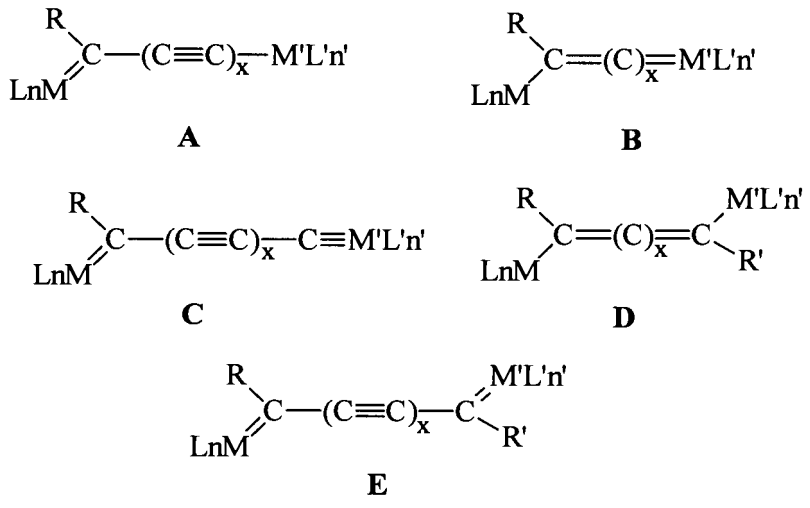

Figure 1.7 Dinuclear complexes with nonlinear conjugated spacers

A feature common to the complexes with linear conjugated spacers and those with nonlinear conjugated spacers, is the M-C(sp^2) linkage of the bridge to both L_nM fragments. They are also models for possible intermediates in the Fischer-Tropsch process[17] and hydrocarbon chemisorbed on metal surfaces[20].

Recently a dinuclear metal complex with a rigid and linear bridging ligand that contains an adamantane spacer was synthesized by Belser *et al.*[21]. Interesting observations were noted. Firstly, it was found that the life time of the intermediate electron transfer product Ru^{II}-PAP-Os^{II} is very long (130μs). Secondly, for the first time in a dinuclear Ru/Os system, it was found that the rate of energy transfer from the Ru^{II} to the Os^{II} unit is faster than the rate of electron transfer from Ru^{II} to the Os^{III} unit.

[20] H.Wadepohl, Angew.Chem.Int.Ed.Engl., 1992, 31, 247.

[21] P.Belser, S.Bernhard, C.Blum, A.Beyeler, L.De Cola, V.Balzani, Coord.Chem.Rev., 1999, 190 -192, 155.

Studies of dinuclear transition metal complexes bridged with π-conjugated groups can help to explain the extended dπ-pπ interaction between transition metals and π-conjugated groups[22].

1.3 CARBENE COMPLEXES

Carbene complexes have a formal metal to carbon double bond. The initial report by Fischer and Maasböl[23] of the targeted synthesis and structural characterization of transition metal carbene complexes in 1964 laid the foundation for a field in organometallic research which has attracted many reseach groups from virtually all branches of inorganic and organic chemistry. There are two bonding extremes for carbene complexes represented by the electrophilic, heteroatom stabilized "Fischer" carbene complexes and the nucleophilic, alkylidene "Schrock" carbene complexes. They are quite different in their behavior and reaction chemistry.

Fischer carbene complexes, a mono- and dinuclear complex are represented in fig.1.8 and Schrock carbene complexes are represented in fig1.9. According to E.O.Fischer[24b] carbene complexes can be prepared from non-carbene complex precursors and by modification of pre-existing carbene complexes. Carbene complexes that can be obtained from non-carbene (carbonyl, allyl, etc) complex precursors can be synthesized from two different methods: (i) transformation of a non carbene ligand into a carbene ligand and (ii) addition of a carbene ligand precursor to a metal complex. From pre-existing carbene complexes, five reactions are possible. They are (i) the transfer of a carbene ligand from one metal center to another, (ii) modification of the carbene ligand, (iii) insertion of an unsaturated organic molecule into the metal carbene bond, (iv) change of the oxidation state of the central metal and (v) modification of the metal-

---

[22] (a) H.Ogawa, T.Joh, S.Takahashi, K.Sonogashira, J.Chem.Soc.,Chem.Commun.1985.1220.
(b) H.Ogawa, K.Onitsuka, T.Joh, S.Takahashi, Organometallics, 1988, 7, 2257.
(c) K.Sonogashira, S.Kataoka, S.Takahashi, N.Hagihara, J.Organomet.Chem., 1978, 160, 319.
(d) A.Wong, P.C.Kang, C.D.Tegge, D.R.Leon, Organometallics, 1990, 9, 1992.
(e) W.-D.Muller, H.A.Brune, Chem.Ber., 1986.119.759.

[23] E.O.Fischer, A.Maasböl, Angew.Chem., 1964, 76, 645.

ligand framework. Metal carbene complexes are known to undergo a variety of reactions and are utilized especially in organic synthesis[24].

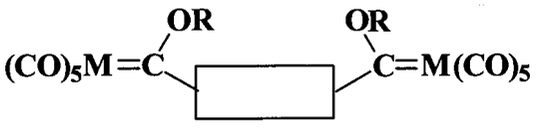

1

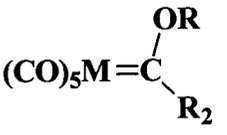

2

Figure 1.8 Fischer carbene complexes

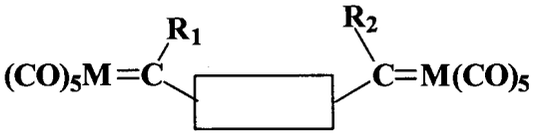

3

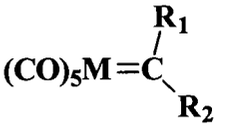

4

Figure 1.9 Schrock carbene complexes

[24] (a) L.S.Hegedus, "Transition metal in the synthesis of complex organic molecules", University Science Book, Mill Valley, California, 1994.

(b) K.H.Dötz, H.Fischer, P.Hofmann, F.R.Kreissl, K.Weiss, "Transition metal carbene complexes", Verlag Chemie, GmbH, D-6940 Weinheim, 1983.

(c) W.D.Wulff, P.-C.Tang, K.-S.Chan, J.S.McCullum, D.C.Yang, S.R.Gilbertson, Tetrahedron, 1985, 41, 5813.

(d) H.-U.Reissig, Organomet.Synthesis, 1989, 2, 311.

The metal in Fischer-type carbene complexes is usually in a low oxidation state, and such a carbene is often stabilized by a heteroatom X, where X = N, O, or S. On the contrary, in the Shrock carbene complexes the metal is often in a high oxidation state. In Fischer-type carbenes, the natures of the metal-carbene carbon bond and the C-X bond in the carbene fragment of the ligand : C(XR')R, are of special interest. Due to the lone-pair electrons of the heteroatom X, the possible π-bond delocalization between M-$C_{carbene}$ and X-$C_{carbene}$ bonds could be formulated as a hybrid of different resonance structures shown as **a-c** in figure 1.10.

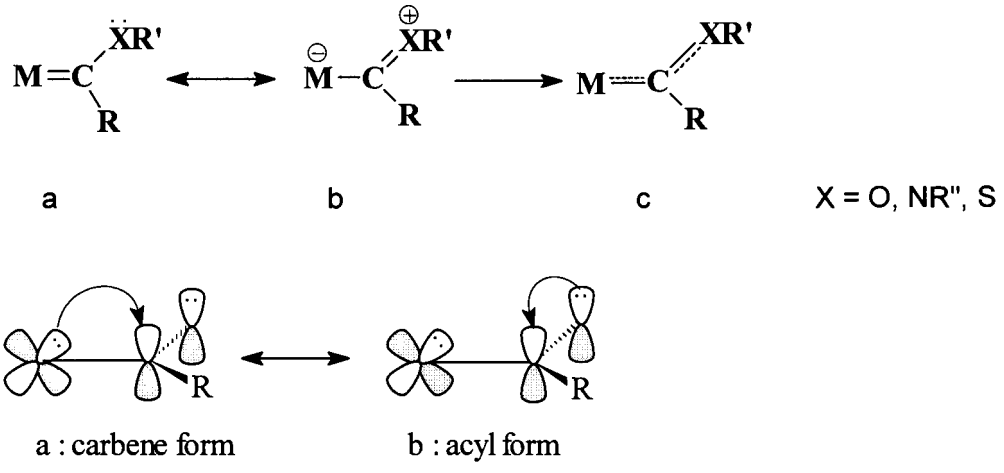

Figure 1.10 Charge delocalization around the carbene-carbon in Fischer carbene complexes

It has been reported by Taylor and Hall[25], that the Fischer-type M-C bond comprises a dative bond between two singlet fragments, depicted **d**, whereas the latter case (Schrock-type) M-C bond is seen as a covalent bond between two triplet fragments, depicted as **e** in figure 1.11.

[25] T.E.Taylor, M.B.Hall, J.Am.Chem.Soc., 1984, 106, 1576.

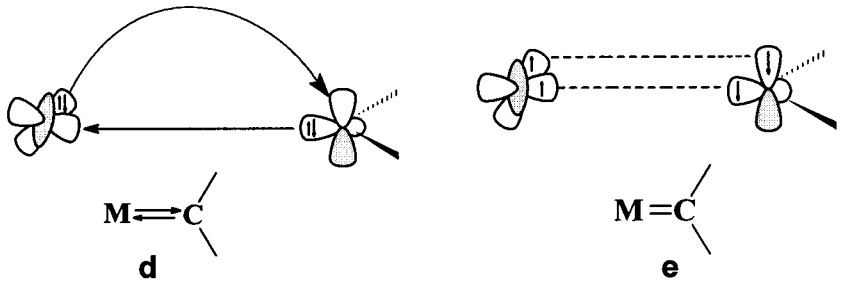

Figure 1.11 M-C bonding in Fischer and Schrock carbene complexes

1.4 THIOPHENE DERIVATIVES AND RELATED COMPOUNDS

Thiophene is the heteroaromatic unit which displays the strongest conductive properties known today[12a]. It has been shown by electrochemical studies that metal-metal interaction in thiophene bridged complexes is weak but greater than in the corresponding phenylene analogues[9].

Dinuclear carbene complexes containing a π-conjugated bridge such as thiophene and its derivatives are attractive compounds to study for the physical and chemical properties they display[3]. Thiophene derivatives are very interesting ligands in coordination chemistry, displaying novel structures and reactivity patterns. Thiophenes display aromatic behavior and can coordinate to metals in different ways as illustrated in figure 1.12.

The interaction of thiophene with transition metal complexes has been studied recently as a model for the heterogeneous hydrodesulfurization (HDS) of petroleum and other fossil fuels[4, 26].

[26] (a) R.J.Angelici, Acc.Chem.Res., 1988, 21, 387.
(b) T.B.Rauchfuss, Prog.Inorg.Chem., 1991, 39, 259.
(c) S.Harris, Organometallics, 1994, 13, 2628.

A number of different reactions and conductivity modes for thiophene have been reported in various metal systems[27] and proposed as molecular analogues for the chemisorption of such sulfur heterocycles onto active metal sites in catalytic surfaces[28]. These include S-coordination, η^2-, η^4- and η^5-coordination, as well as some bridging modes in dinuclear cluster compounds. Several of these bonding modes have been suggested to be associated with reaction steps of HDS processes like hydrogenation[29], hydrogenolysis[30] and complete desulfurization. It has been reported recently by Jones and coworkers[29b] that both C-H and C-S insertion occur when $(C_5Me_5)Rh(PMe_3)(Ph)H$ is irradiated at low temperatures in the presence of thiophene and the C-S insertion product was identified as $Rh(C_5Me_5)(PMe_3)(SCH{=}CHCH{=}CH)$.

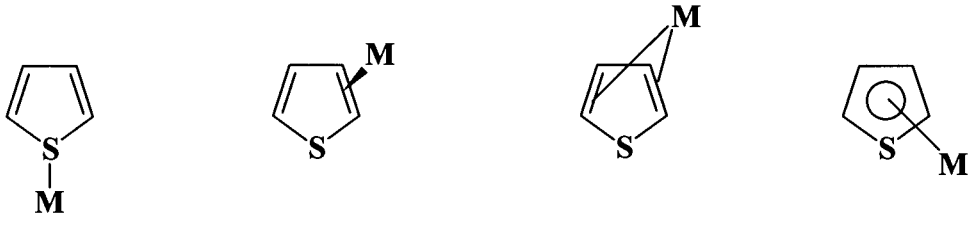

S-coordination η^2-coordination η^4-coordination η^5-coordination

Figure 1.12 Coordination modes of thiophene to a metal.

[27] (a) M.G.Choi, M.J.Robertson, R.J.Angelici, J.Am.Chem.Soc., 1991, 113, 4005.
(b) J.Chen, Y-Su, R.A.Jacobson, R.J.Angelici, J.Organomet.Chem.,1992, 428.

[28] C.Bianchini, A.Meli, M.Peruzini, F.Vizza, V.Herrera, R.S.Sanchez-Delgado, Organometallics, 1994, 13, 721.

[29] (a) D.A.Lesch, J.W.Jr.,Richardson, R.A.Jacobson, R.J.Angelici, J.Am.Chem.Soc., 1984, 106, 2901.
(b) W.D.Jones, L.Dong, J.Am.Chem.Soc., 1991, 113, 559.

[30] C.Bianchini, A.Meli, M.Peruzzini, F.Vizza, P.Frediani, V.Herrera, R.S.Sanchez-Delgado, J.Am.Chem.Soc., 1993, 115, 2731.

When 2,5-trimethylstannyl-substituted thiophenes and chloro complexes are employed, oligothiophene bridged complexes **A** in figure 1.13 are formed[14] which are of interest due to the electrical conductivity of polythiophenes [8a,b].

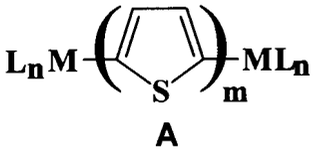

A

ML_n = $Ru(CO)_2Cp$

= $Pt(PBu_3)_2Cl$

m = 1, 2, 3

Figure 1.13 Dinuclear oligothiophene complex

1.5 Aim of this study

Thiophene and bithiophene represent very interesting ligands in coordination chemistry displaying novel structures and reactivity patterns[4,31,28,29c]. In this study we extended the promising results obtained for bithiophene[32] to the corresponding trimer of thiophene.

The synthesis[33] and characterization[28] of terthienyl have been documented. The metallation of the trimeric oligothiophene was investigated, used as a reagent to react with metal carbonyls with the purpose of forming a spacer unit in binuclear biscarbene complexes.

---

[31] (a) A.du Toit, M.Landman, S.Lotz, J.Chem.Soc., Dalton Trans., 1997, 2955.
(b) T.A.Waldbach, P.H.van Rooyen, S.Lotz, Angew.Chem.Int.Ed.Engl., 1993, 32, 710.
(c) T.A.Waldbach, R.van Eldik, P.H.van Rooyen, S.Lotz, Organometallics, 1997, 16, 4056.

[32] M.van Staden, Unpublished results.

[33] (a) S.K.Tamao, S.Kodama, I.Nakajima, M.Kumada, Tetrahedron, 1982, 38, 3347.
(b) A.McEachern, C.Soucy, L.C.Leitch, J.T.Arnason, P.Morand, Tetrahedron, 1998, 44, 2403.
(c) J.Kagan, S.K.Arora, J.Org.Chem., 1983, 48, 4317.

In our laboratory we discovered that σ,π-bonded thiophene facilitates a unique metal exchange reaction whereby the metals irreversibly exchange coordination sites[31b]. Furthermore, unique properties of reactivity were also observed when [Cr(η^5-C_5H_4S)$(CO)_3$] was metallated and reacted with metal carbonyls.[31c]

The stability and reactivity of dinuclear biscarbene complexes with thiophene spacer units have been investigated and this work was extended to include condensed thieno [3,2-b] thiophene units.[3a,3c]

A marked increase in the stability of biscarbene complexes with bithiophene spacer substituents was recently observed which raised the question whether three thiophene rings could (i) further stabilize biscarbene complexes, (ii) still display π-delocalization over the extended spacer and (iii) reveal novel structural features and reaction patterns.

In this study the synthesis and properties of carbene complexes with terthienyl substituents were addressed. The effect of the increase in length of the bridging ligand compared to shorter thiophene spacer units, stability of the complexes, possible metal communication through the spacer and their aminolysis reactions were studied. (Figure 1.14)

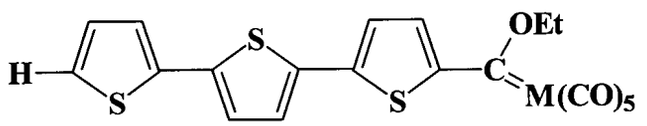

A

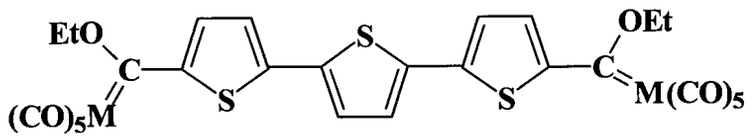

B

M = W, Cr and Mo

Figure 1.14 Ethoxy(terthienyl)carbene complexes

CHAPTER 2

TERTHIENYL

2.1 Introduction

Recently, naturally occurring thiophene derivatives such as HTTTH have received a great deal of attention because of their phototoxic activity[1] and their conductivity[2]. Studies on the fundamental photochemical studies[3] have shown that HTTTH is an efficient singlet oxygen generator, toxic to a number of target organisms[4]. HTTTH has demonstrated potent insecticidal activity, making it excellent for ongoing evaluation.

HTTTH was synthesized in order to examine its potential for charge transfer in a π-delocalized system and its physical properties as a spacer in carbene complexes. Thus providing information that can be useful to design more efficient molecular wires, liquid crystals and optical materials.

More than fifty five years ago Steinkopf and coworkers[5] obtained oligomers with 2 to 7 thiophene units by heating 2-iodothiophene with copper bronze or through copper promoted coupling of 2,5-diiodothiophene with 2-iodothiophene. This method was not successful because mixture of the oligomeric species, which were difficult to separate, were obtained.

---

1 G.H.N.Towers, Can.J.Bot., 1984, 62, 2900.

2 (a) J.Roncali, Chem.Rev., 1992, 92, 711.

(b) A.O.Patil, A.J.Heeger, F.Wudl, Chem.Rev., 1988, 88, 183.

3 J.C.Scaiano, A.McEachern, J.T.Arnason, O.Morand, D.Weir, Photochem.Photobiol., 1987, 46, 193.

4 J.R.Heitz, K.R.Downum Ed., Am.Chem.Soc.Washinton D.C., 1987, Chapter 18, 255.

5 (a) W.Steinkopf, H.J.V.Peterstorff, R.G.Gording, Justus Liebigs Ann.Chem., 1937, 527, 272.

(b) W.Steinkopf, R.Leitsman, K.H.Hofmann, ibibi., 1941, 546, 180.

Several syntheses of HTTTH are reported in literature[6], including a small scale nickel-catalyzed cross-coupling reaction by Kumada *et al.*[7] In a recent article[8] all of these methods were reported and discussed in some detail. HTTTH has three conformers based on the position of sulfur atoms with respect to the interfering bond. All *cis* (a), *cis-trans* (b) and all *trans* (c) are possible.

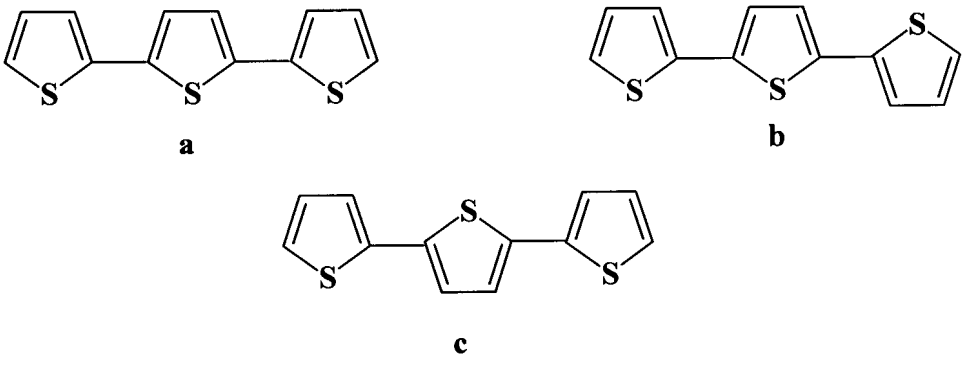

Figure 2.1 Conformers of HTTTH

It has been reported by van Pham *et al.*[9] that the all *trans* arrangement is the predominant conformer in solution. It has also been found that the latter form (c) has the lowest dipole moment[10], and consequently it should be less affected by solvent polarity. In our study we obtained the all *trans* (c) as it is shown in the crystallographic structure of the biscarbene complex (ball and stick) in figure 3.18 (chapter 3). By 1989, the longest thienylene oligomer synthesized had six thiophene rings[9].

---

[6] (a) J.Kagan, S.K.Arora, J.Org.Chem., 1983, 48, 4317.
(b) J.Kagan, S.K.Arora, Heterocycles, 1983, 20, 1941.
(c) T.Asano, S.Ito, N.Saito, K.Hatakeda, Heterocycles, 1977, 6, 317.
(d) J.Kagan, S.K.Arora, Tetrahedron Lett., 1983, 24, 4043.

[7] S.K.Tamao, S.Kodama, I.Nakajima, M.Kumada, Tetrahedron, 1982, 38, 3347.

[8] J.Nakayama, T.Konishi, M.Hoshino, Heterocycles, 1988, 27, 1731.

[9] C.van Pham, A.Burkhardt, R.Shabana, D.D.Cunningham, H.B.Mark, jr., H.Zimmer, Phosphorus, Sulphur, and Silicon, 1989, 46, 153.

[10] R.H.Abu-Eittah, F.A.Al-Sugar, Bull.Chem.Soc.Jpn., 1985, 58, 2126.

2.2 Synthesis

The Michael addition of aldehydes to α,β-unsaturated ketones (or Mannich base precursors) developed by Stetter[11] has been applied to the synthesis of 1,4-diketone containing one thiophene ring in the presence of cyanide ions as catalyst[5].

3-Dimethyl-amino-1-(2-thienyl))-propanone was afforded by refluxing a mixture of 2-acetylthiophene, paraformaldehyde, dimethylamino.HCl and concentrated HCl in 95% ethyl alcohol for 16 hours. Cooling produced the hydrochloride of the Mannich base. The hydrochloride of the Mannich base was made alkaline with ammonia solution and extracted three times with ether. Washing and drying of the ether layer, followed by evaporation of the solvent afforded the white crystalline Mannich base complex which was used at once in the synthesis of 1,4-bis(2-thienyl)-1,4-butanedione.

2-Thiophene aldehyde was allowed to react with 3-dimethyl-amino-1-(2-thienyl)-propanone in dry DMF in the presence of NaCN. The mixture was left overnight and the solution turned yellowish-green in colour. Water was added and the solution was extracted three times with chloroform. The chloroform layer was washed and dried on $MgSO_4$. Removal of the solvent and recrystallization from hot ethanol afforded shiny white crystals of the diketone in high yield. The diketone was cyclized by reacting it with P_2S_5 in the presence of $NaHCO_3$. High yields of terthienyl were obtained. The product was purified with column chromatography and recrystallized with ethanol. A yellowish product with a melting point in the range 94-95 °C was characterized as terthienyl. The reaction scheme is outlined in figure 2.2.

[11] (a) H. Wynberg, J. Metselaar, Synth.Commun., 1984, 14, 1.
(b) H. Stetter, Angew.Chem.Int.Ed.Engl., 1976, 15, 639.
(c) H. Stetter, H. Bender, Angew.Chem., 1978, 90, 130.

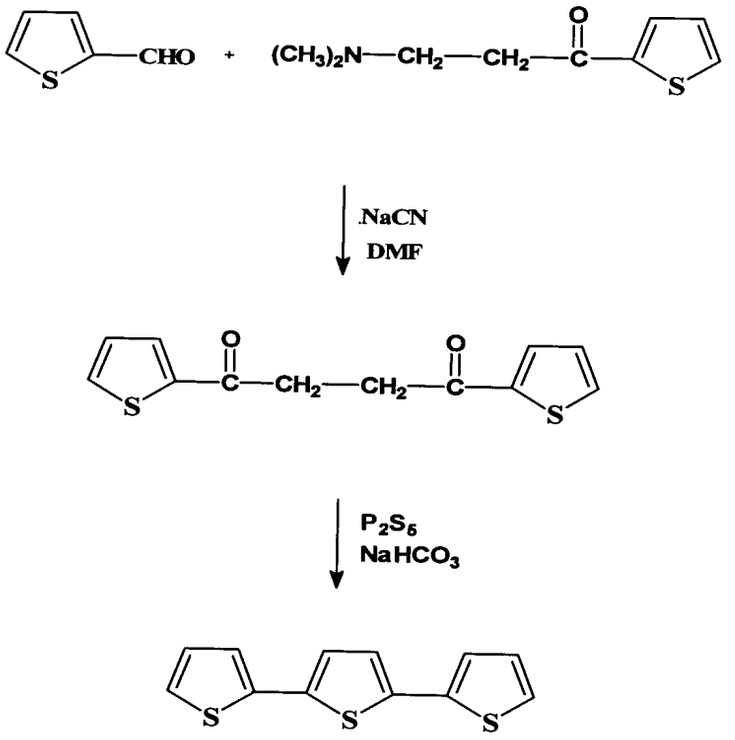

Figure 2.2 Procedure for preparation of HTTTH

2.3 Characterization

HTTTH was characterized with UV-visible, ^{1}H NMR-, ^{13}C NMR-spectroscopy, and a 2D HETCOR experiment helped in assigning resonances.

2.3.1 ^{1}H NMR spectroscopy

The NMR spectra were recorded in $CDCl_3$ solvent as reference. The numbering of the carbon atoms of the HTTTH rings is shown in figure 2.3 and this numbering was followed when assigning the proton and carbon-13 spectra.

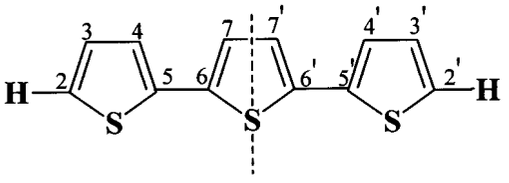

Figure 2.3 Atom numbering of HTTTH

The data of the ^{1}H NMR spectra of HTTTH are summarized in table 2.1. The ^{1}H NMR spectrum for HTTTH is represented by figure 2.4.

Table 2.1 ^{1}H NMR data of HTTTH complex

Proton	δ, (ppm)	J_4, (Hz)	J_3, (Hz)	Signal
H2, H2'	7.20	1.14	5.16	dd
H4, H4'	7.16	1.14	3.63	dd
H3, H3'	7.00		5.13, 3.63	2xd
H7, H7'	7.06	-	-	s

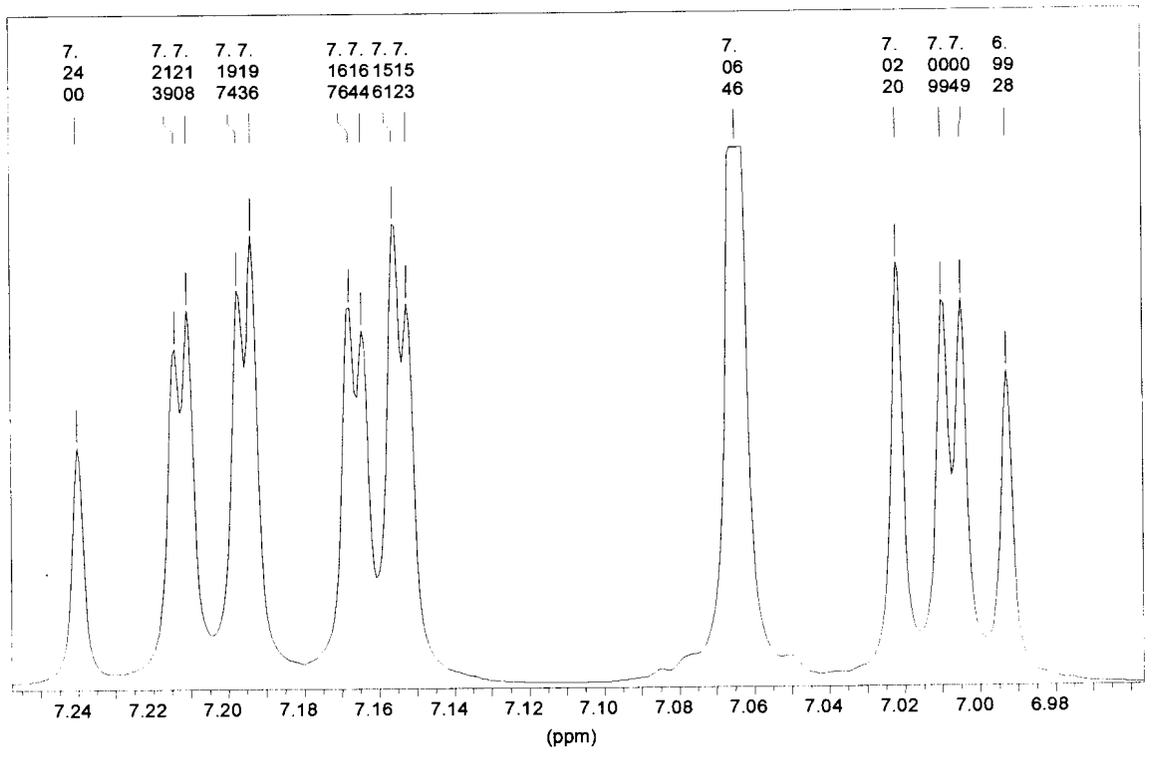

Figure 2.4 ^{1}H NMR Spectrum of HTTTH

HTTTH protons resonated in the region between 6.99 ppm and 7.24 ppm as shown in figure 2.4. They display a downfield shift. This is because of their deshielding due to the diamagnetic anisotropy generated by the π-electrons of the double bonds. HTTTH exhibits aromatic behavior.

Only four sets of signals are observed from the spectrum in figure 2.4. There are two doublet of doublets (dd), a double doublet (2xd) and a singlet. Evaluation of the proton spectrum and the coupling constants on the ^{1}H NMR shows that the complex is symmetrical and the data in table 2.1 corresponds well with the observation by McEachern *et al*[12].

[12] A. McEachern, C. Soucy, L. Leitch, J.T. Arnason, P. Morand, Tetrahedron, 1988, 44, 2405.

The doublet of doublets at 7.20 ppm is assigned to H2/2' since these are mostly affected by the diamagnetic anisotropy generated by the π-electrons of the double bonds and are bonded to a carbon adjacent to the sulfur atom. A double doublet at 7.00 ppm is assigned to H3/3' and the doublet of doublets at 7.16 ppm is assigned to H4/4'. A singlet at 7.06 ppm is assigned to the H7/7' protons because they are equivalent by symmetry i.e. magnetically equivalent. The coupling constants J_3 and J_4 also fit in with those reported by McEachern *et al*[6].

The splitting patterns of the interacting nuclei H2/2', H3/3' and H4/4' are shown in figure 2.5. The three nuclei have different chemical shifts. Each nuclear signal is split by coupling with both the other nuclei, i.e. H2/2' is split into a doublet of separation J_3 by H3/3' and further split into a doublet of separation J_4 by H4/4'. Thus each nucleus gives a four signal pattern shown in figure 2.4. The long range coupling represented by J_4 is weaker than the vicinal couplings represented by J_3 since it occurs over a larger distance.

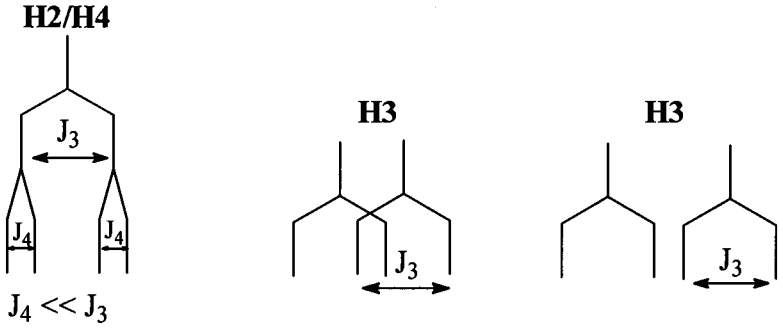

Figure 2.5 Analysis of the splitting pattern in figure 2.4

2.3.2 ^{13}C NMR spectroscopy

The ^{13}C NMR-spectral data of HTTTH are summarized in table 2.2 and a selected region of the spectrum is represented in figure 2.6.

HTTTH consist of eight protonated carbons, but due to its symmetry, gives rise to four intense signals in the aromatic region as displayed in figure 2.6. In addition to these there are four quartenary carbons with longer relaxation times i.e. showing low

intensities as expected. These afford only two signals in the region 136 ppm to 138 ppm because of the symmetry centre in the molecule.

Assignment of these signals to their respective carbons was done using the HETCOR diagram in figure 2.7. Of all the aromatic signals, C5" was the most deshielded at 128.5 ppm because of the electronegative heteroatom (S) bonded to it.

Table 2.2 ^{13}C NMR data for HTTTH

Carbon	δ (ppm)
C5, C6	137.8, 136.8
C3/3'	129
C2/2'	125.2
C7/7'	124.9
C4/4'	124.4

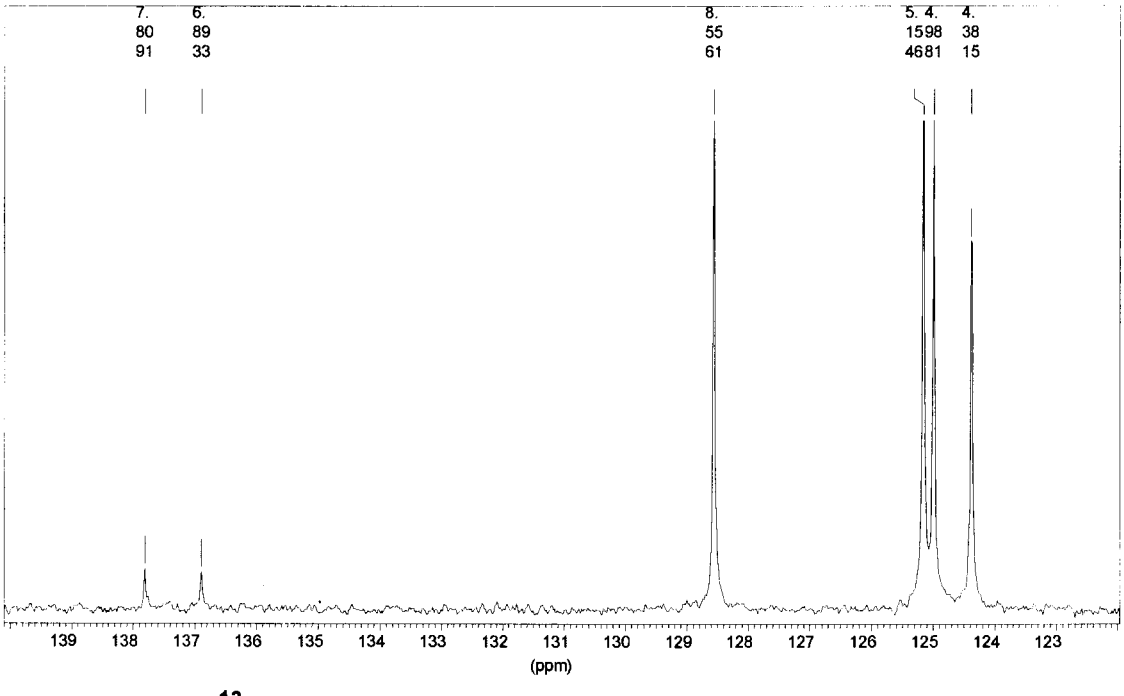

Figure 2.6 ^{13}C NMR Spectrum of HTTTH

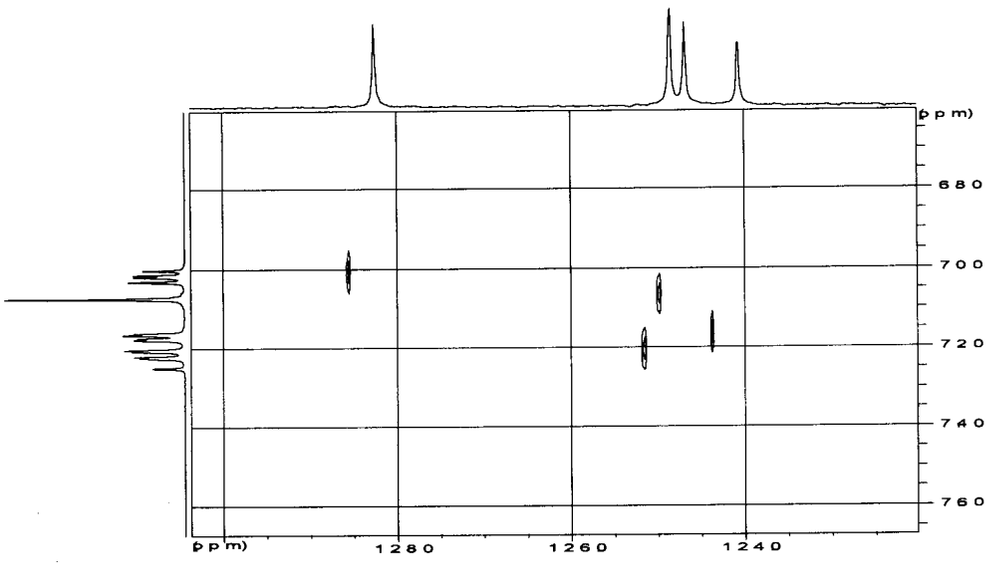

Figure 2.7 HETCOR diagram of HTTTH

2.3.3 UV Spectroscopy

The UV-spectrum of HTTTH is represented by figure 2.8. From its spectrum, the wavelength of the purple light is absorbed thus transmitting the yellow colour of the substrate. There are two bands of medium intensity above 200 nm characteristic of the aromatic system. The third band at 217 nm indicates the presence the of polyaromatic system in HTTTH. HTTTH has a strong absorption band at 331 nm, 343 nm characteristic for the π-π^* interband transitions of the entire chromophore[13]. The less intense band may also be due to the π-π^* local excitation transitions of the heteronucleus[14]. The λ-max of unsubstituted oligothiophenes increases with the number of thiophene units in the chain.

[13] J.Murrel, J.Chem.Soc., 1956, 3779.

[14] R.F.Curtis, G.T.Phillips, Tetrahedron, 1967, 23, 4419.

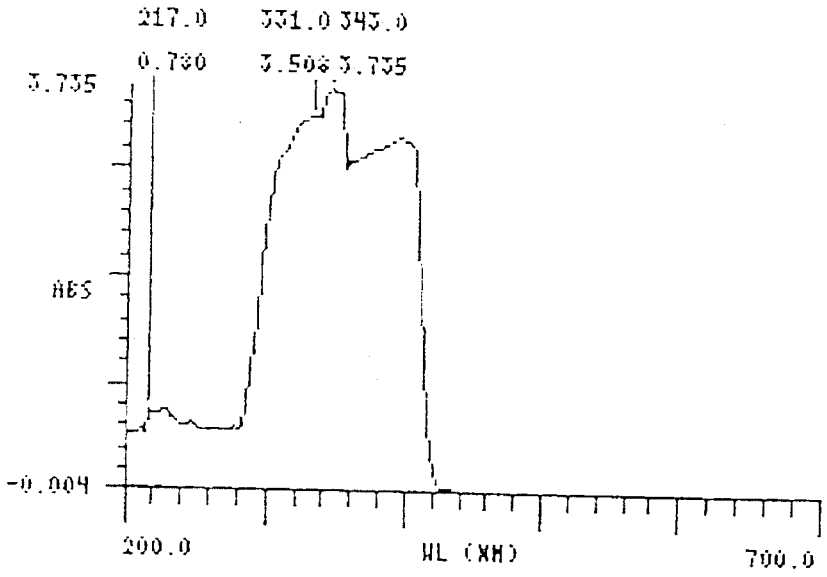

Figure 2.8 UV-Spectrum of HTTTH

2.3.4 Conclusion

Terthienyl was successfully synthesized using the method described. A yellowish product stable in air was obtained. Terthienyl was fully characterized with NMR spectroscopy and data corresponds to the results obtained earlier[8]. Structural evidence revealed that the *all trans* conformer was obtained. Ultraviolet spectroscopy data also revealed π-delocalization in terthienyl as already explained in literature[2].

CHAPTER 3

ETHOXYCARBENE COMPLEXES

3.1 Introduction

Fischer carbene complexes have received much attention since the synthesis of $[W(CO)_5C(OMe)Ph]$ by Fischer and Maasböl[1]. Phenyl and dinuclear biphenylene carbene complexes in figure 3.1 were the first types of aromatic carbene complexes reported[1]. Crystallographic data reported in the same article showed that the biphenylene biscarbene complex was centrosymmetric whereas for biphenyl derivatives coplanar structures were observed.

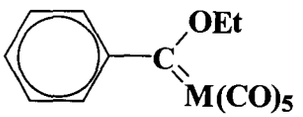

M = Cr
M = W

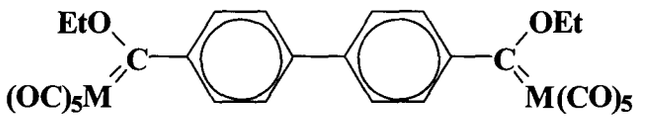

M = Cr
M = W

Figure 3.1 Phenyl and dinuclear biphenylene carbene complexes

Because of the interesting physical properties they exhibited, C_n carbon rich[2], aromatic[3] and heteroaromatic[4] carbene complexes prompted further investigation.

---

[1] E.O.Fischer, A.Maasböl, Angew.Chem., 1964, 76, 645.

[2] (a) W.Beck, B.Niemer, M.Wieser, Angew.Chem.Int.Ed.Engl, 1993, 32, 923.

(b) H.Lang, Angew.Chem.Int.Ed.Eng., 1994,34,547.

(c) T.Bartik, W.Weng, J.A.Ramsden, S.Szafert, S.B.Falloon, A.M.Arif, J.A.Gladysz, J.Am.Chem.Soc., 1998, 120, 11071.

[3] N.Hoa Tran Huy, P.Lefloch, Y.Jeannin, J.Organomet.Chem., 1987, 327, 211.

[4] (a) Y.M.Terblans, H.M.Roos, S.Lotz, J.Organomet.Chem., 1998, 566, 133.

(b) M.Landman, H.Görls, S.Lotz, J.Organomet.Chem., 2001, 285, 617.

(c) M.Landman, H.Görls, S.Lotz, Eur.J.Inorg.Chem., 2001, 233.

Thiophene derivatives are receiving much attention as conductive polymers[5]. Thiophene units are the heteroaromatic units that display the strongest conductive properties known today[6], hence the utilization of the heteroaromatic substrates as spacer units between two carbene ligands.

Recently, mono and biscarbene (figure 3.2) complexes of thiophene [4a,6], bithiophene[7], condensed thiophene rings[4] with group 6 transition metals and their decomposition products were synthesized in our laboratories and studied extensively. Because of their interesting structural and electronic features, it was decided to extend this work to the mono- and biscarbene complexes of the thiophene trimer.

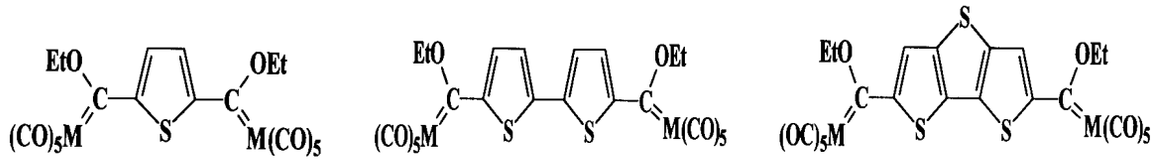

Figure 3.2 Thiophene derived biscarbene complexes

These systems all have in common conjugated, delocalized moieties capable of distributing electron density from one end of the molecule to the other. It has been shown recently by electrochemical studies that metal-metal communication in thiophene bridged complexes is weak but greater than in the corresponding phenylene analogues[8].

---

[5] (a) J.Nakayama, T.Konishi, Heterocycles, 1988, 27, 1731.
(b) A.Amer, H.Zimmer, K.J.Mulligan, H.B.Mark Jr., S.Pons, J.F.McAleer, J.Polym.Sci.Polym.Lett.Ed., 1984, 22, 77.

[6] Y.M.Terblans, PhD Theses, Thiophene Bimetallic Carbene Complexes, 1996.

[7] M.van Staden, MSc dissertation, Binuclear bithiophene Biscarbene Complexes (unpublished results), University of Pretoria.

[8] K.R.Justin Thomas, J.T.Lin, Yu S.Wen, Organometallics, 2000, 19, 1008.

Carbene complexes of chromium, tungsten, and molybdenum with terthienyl substrates were synthesized and their stabilities compared.
Preparation of terthienyl carbene complexes of group 6 metals involves two steps: addition of lithiated terthienyl (LiTTTLi(H)) to a metal carbonyl followed by conversion of the resulting metalacylates to the corresponding alkoxy carbene complexes.

Thiophene and its derivatives are readily monolithiated by butyllithium in THF and dilithiated in the absence of THF and it has been established sometime ago that these reactions are almost quantitative[9]. It was found that the BuLi:TMEDA complex was a prerequisite for the efficient dilithiation of thiophene derivatives. Metallation of thiophene and its derivatives occurs exclusively at the position α to the heteroatom[10] .

3.2 Synthesis

The procedure similar to that used for the synthesis of thiophene carbene complexes was followed[6a]. The mono- and biscarbene complexes were afforded in one reaction mixture by using two equivalents of n-BuLi in the presence of TMEDA and hexane:THF mixture during lithiation. The reaction was carried out under an inert atmosphere of nitrogen.

The reaction scheme for the synthesis of carbene complexes is shown in scheme 3.1. The reaction afforded two products. Based on full characterization, it was concluded that the reddish-brown product is the terthienyl monocarbene complex and the purple-blue product is the terthienyl biscarbene complex.

[9] (a) H. Gilman, D.A. Shirley, J.Am.Chem.Soc., 1949,71, 1870.
(b) L.N. Koikov, N.V. Alekseeva, M.A. Polikarpov, K.F. Turchin, Organomet.Chem, U.S.S.R., 1991, 4, 664.

[10] S.L. Graham, T.H. Scholz, J.Org.Chem.,1991,56,4260.

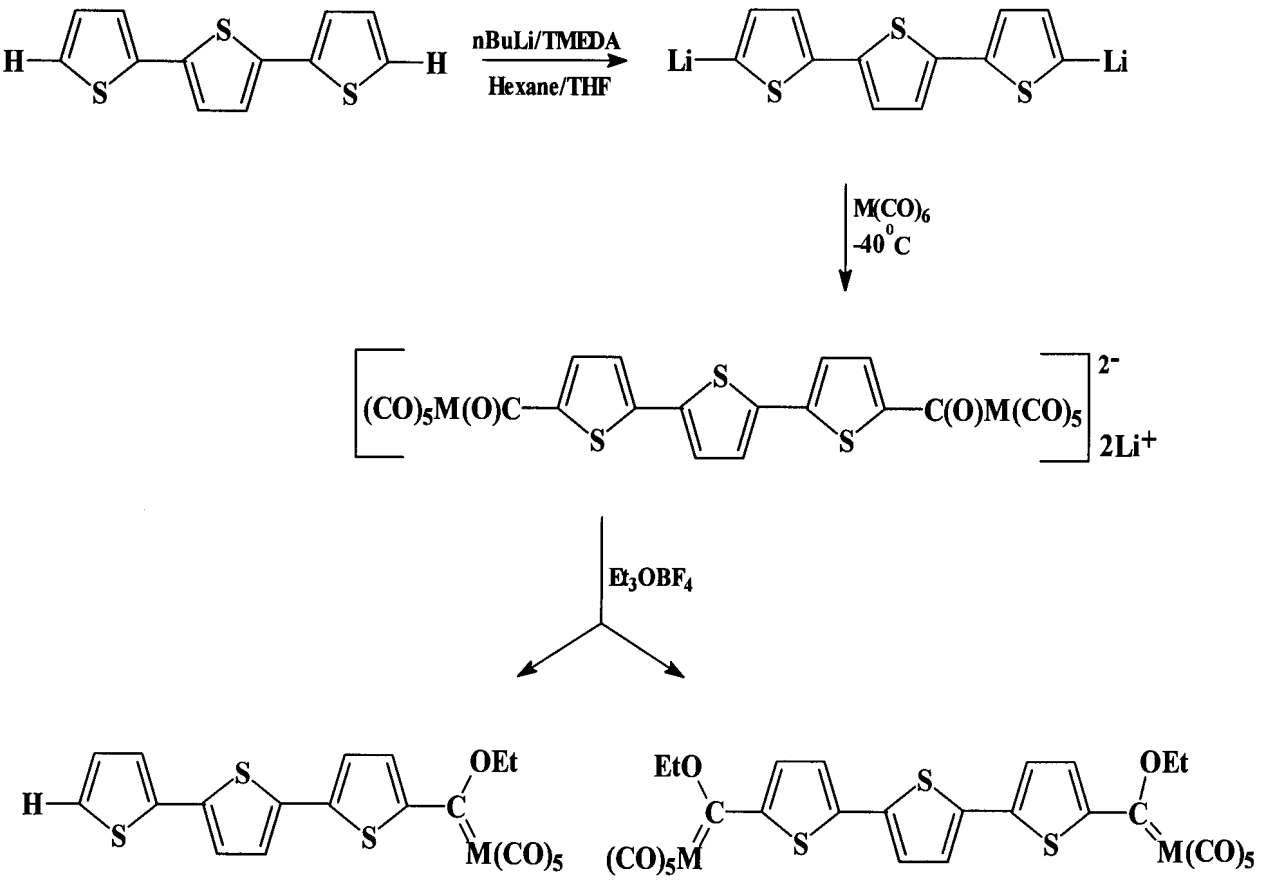

Monocarbene

M = Cr (**2**), Mo (**3**) and W (**4**)

Biscarbene

M = Cr (**5**), Mo (**6**) and W (**7**)

Scheme 3.1 Formation of complexes 2-7

3.3 Monocarbene complexes

3.3.1 Spectroscopic characterization of carbene complexes 2- 7

Both the mono- and biscarbene complexes were characterized with NMR spectroscopy (^1H, ^{13}C) and assignments confirmed with 2D HETCOR and COSY experiments, infrared spectroscopy and mass spectrometry. UV- visible spectroscopy was also used to study metal-metal communication. The structure of the complex was confirmed with the help of single crystal X-ray diffraction studies.

3.3.1.1. ^1H NMR spectroscopy

NMR samples were prepared under inert atmosphere and all the spectra were recorded in deuterated chloroform.

The data of the ^1H NMR spectrum for the monocarbene complexes **2-4** are summarized in table 3.1.

Table 3.1 ^1H NMR data of complexes 2 to 4

Protons	**2**			**3**			**4**		
	δ(ppm)	J_3(Hz)	J_4(Hz)	δ(ppm)	J_3(Hz)	J_4(Hz)	δ(ppm)	J_3(Hz)	J_4(Hz)
H3	**8.17(d)**	**4.2**	-	**8.13(d)**	**4.4**		**8.09(d)**	**4.4**	-
H4	**7.26(d)**	**4.2**	-	**7.26(d)**	**4.4**	-	**7.26(d)**	**4.4**	-
H7	**7.30(d)**	**3.8**	-	**7.32(d)**	**3.8**	-	**7.33(d)**	**3.9**	-
H8	**7.12(d)**	**3.8**	-	**7.12(d)**	**3.8**	-	**7.12(d)**	**3.8**	-
H11	**7.22(dd)**	**3.5**	**1.3**	**7.22(dd)**	**3.6**	**1.3**	**7.22(dd)**	**3.6**	**1.1**
H12	**7.03(dd)**	**3.8, 5.0**	-	**7.04(dd)**	**3.6, 5.2**	-	**7.03(dd)**	**3.6, 4.9**	-
H13	**7.27(dd)**	-	-	**7.27(dd)**	**4.9**	**1.1**	**7.27(dd)**	**5.2**	**1.1**
OCH_2CH_3	**5.05(q)**	**7.05**	-	**5.03(q)**	**7.05**		**4.95(q)**	**7.05**	-
OCH_2CH_3	**1.66(t)**	**7.05**	-	**1.64(t)**	**7.05**		**1.63(t)**	**7.05**	-

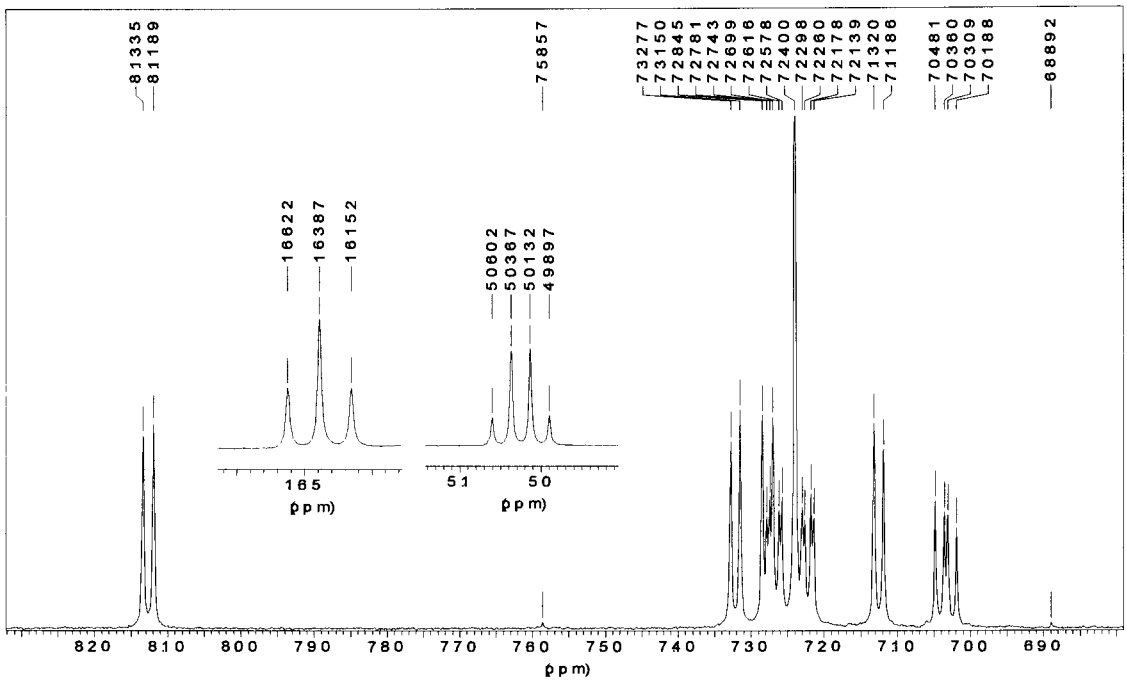

Figure 3.3 ^{1}H NMR spectrum of 3

The ^{1}H NMR spectrum of **3** in figure 3.3 is used as a representative for the three monocarbene complexes **2-4**.

From the representative ^{1}H NMR spectrum of **3** in figure 3.3, it is clear that the protons of the terthienyl substituent are in different environments. Conclusions were made from chemical shift values, coupling constants and a 2D HETCOR experiment. Assignment of protons is based on the atom numbering in figure 3.4.

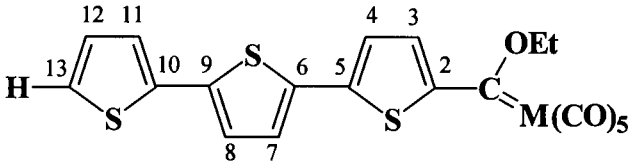

Figure 3.4 Monocarbene Complex with atom numbering

The monocarbene complex in figure 3.4 has seven protons on the terthienyl substituent. The spectrum exhibits seven sets of signals in the region between 7.03 and 8.17 ppm depending on the number of metal substituents or metal itself. There are two doublet of doublets (dd), a double doublet (2xd) and four doublets (d).

Compared to the signals of free terthienyl, these signals are far downfield. The signal at 8.13 ppm is assigned to proton H3. This is because the carbene carbon is highly electrophilic and with the metal pentacarbonyl moiety in Fischer type carbene complexes, which serves as a strong electron-withdrawing group, make the α-protons of the carbene carbon highly deshielded.

The deshielding effect in complexes **2-4** differs slightly, but the effect of each metal is clearly observed. Since the electron density increases down the group, the observed deshielding trend of H3 in complexes **2-4** is $\sigma(\mathbf{2})>\sigma(\mathbf{3})>\sigma(\mathbf{4})$. From this trend one can conclude that the shielding of a proton increases with an increase in atomic number of the metal. Deshielding of protons in these complexes is explained satisfactorily by figure 3.5.

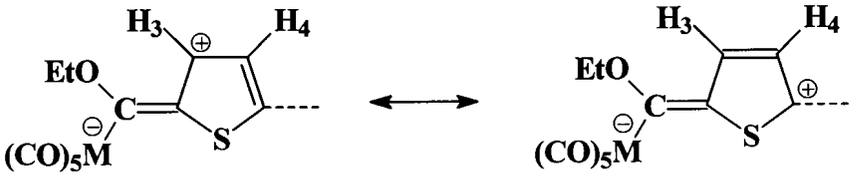

M = Cr
= Mo
= W

Figure 3.5 Charge delocalization in 2-4

The position of the chemical shift of H3 is also supported by the fact that coordinated carbene ligands are strong σ-donors but weaker π-acceptors, hence strong polarization towards the metal is observed leaving closer protons deshielded.

The signal that appears downfield at 7.27 ppm represents proton H13's splitting pattern. The signal is assigned to H13 because it is bonded to the carbon adjacent to the

electronegative sulfur atom. The chemical shift of signals in the range 7.32 to 7.04 ppm for complexes **2-4** are predominately influenced by the diamagnetic anisotropy generated by the π-electrons of the double bonds.

From table 3.2, it is clear that proton H13 of the terminal terthienyl group was only slightly affected. The differences in chemical shift values of the corresponding protons in the complex and terthienyl are small. This implies that the carbene ligand on the other side of terthienyl has little effect on the distant H11 – H13.

Table 3.2 Shift differences between protons of free terthienyl and 3

Proton	Monocarbene Complex	Terthienyl	Difference
H12	7.04 ppm	7.01 ppm	0.03 ppm
H11	7.23 ppm	7.16 ppm	0.07 ppm
H13	7.27 ppm	7.20 ppm	0.07 ppm

From the spectrum in figure 3.3, a doublet is observed in the region 7.26 ppm. This doublet is assigned to H4. H7 is downfield compared to H8 because of the electron drainage from one end of the carbene complexes.

The methylene protons of the ethoxy substituent of the carbene carbon resonated at 5.03 ppm as a quartet and the methyl protons at 1.64 ppm as a triplet.

3.3.1.2 ^{13}C NMR Spectroscopy

The ^{13}C NMR data of the monocarbene complexes **2-4** are tabulated in table 3.3.

Table 3.3 ^{13}C NMR data of complex 2-4

Assignment Carbons	COMPLEXES Chemical Shifts (δ, pm)		
	2	**3**	**4**
C1	311.2	301.9	286.0
CO(trans)	223.4	212.9	202.5
CO(cis)	217.2	206.2	197.7
C2, C5, C6, C9, C10	152.0, 146.6, 139.6, 136.4, 134.6	152.8, 147.6, 139.8, 136.4, 134.6	155.1, 147.7, 139.8, 136.5, 134.8
C3	142.9	143.8	143.8
C7	128.1	128.1	128.1
C13	127.2	127.9	127.2
C11	125.5	125.6	125.6
C4	125.0	124.9	124.9
C8	124.8	124.8	124.8
C12	124.6	124.6	124.6
OCH_2	75.6	77.3	78.1
CH_3	15.2	15.9	15.0

The ^{13}C NMR spectrum of complex **2** in figure 3.7 is representative for the complexes **2-4**.

Carbene carbons of **2-4** resonated in the region ranging from 280 - 330 ppm. This region lies well within the range of values found for carbocations of organic chemistry, thus implying a substantial positive charge on the carbene carbon. This is explained by the canonical forms **A** and **B** in figure 3.9.

The assignment of the carbon-proton signals is done with the help of the HETCOR spectrum in figure 3.8.

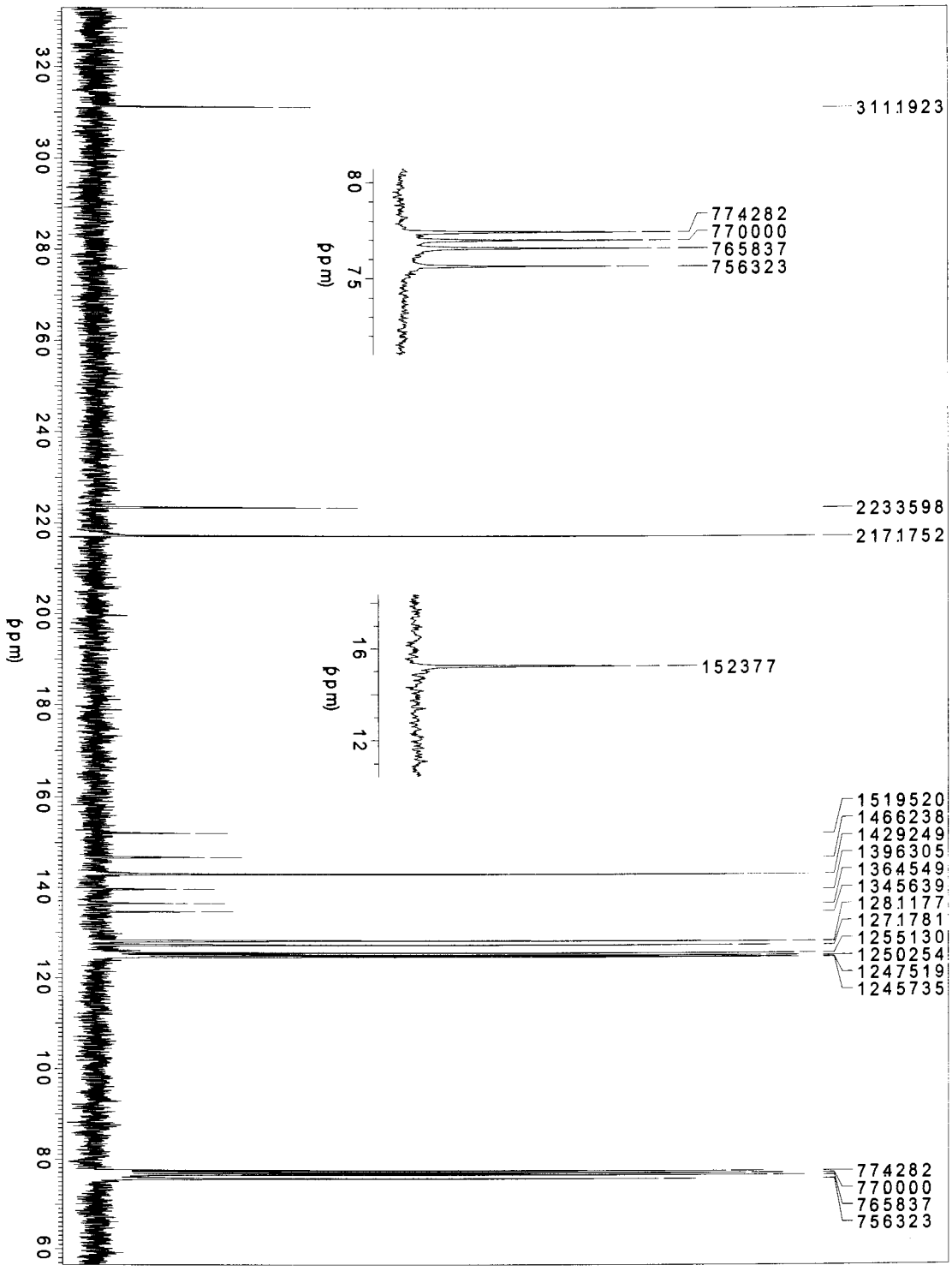

Figure 3.7 ^{13}C NMR spectrum of complex 2

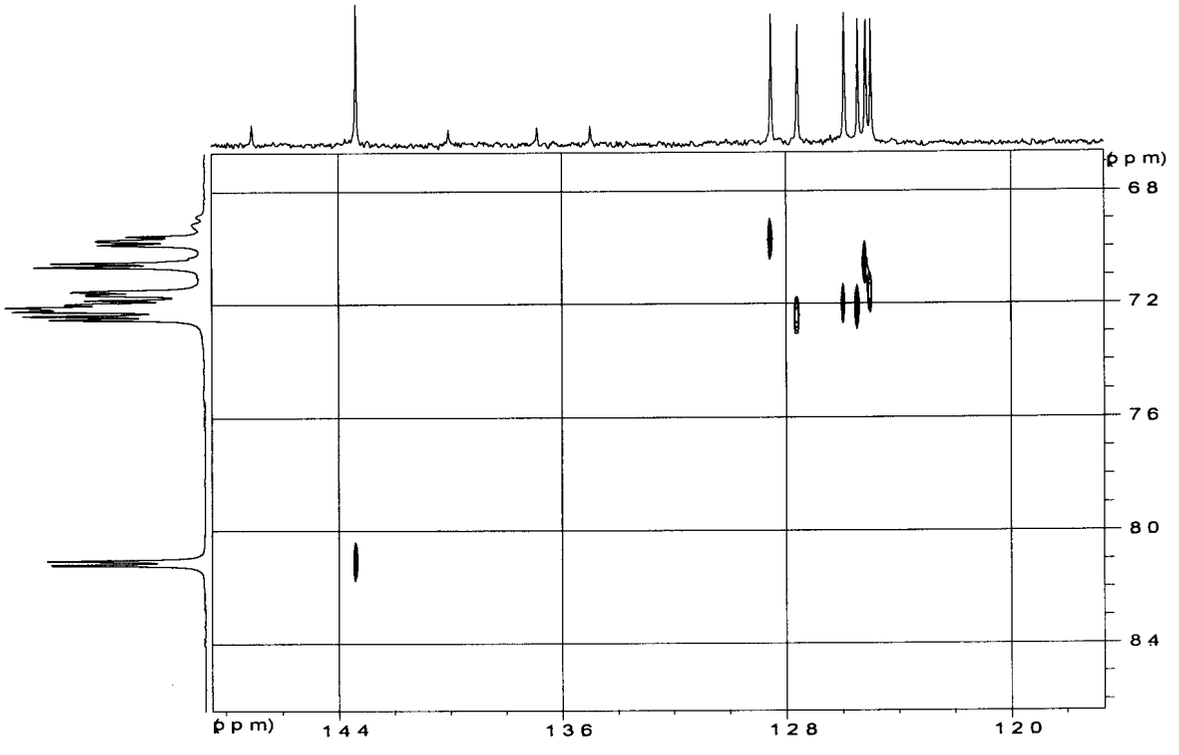

Figure 3.8 2D HETCOR of complex 2

The assignment of the carbene carbons is well explained by the charge delocalization diagram in figure 3.9.

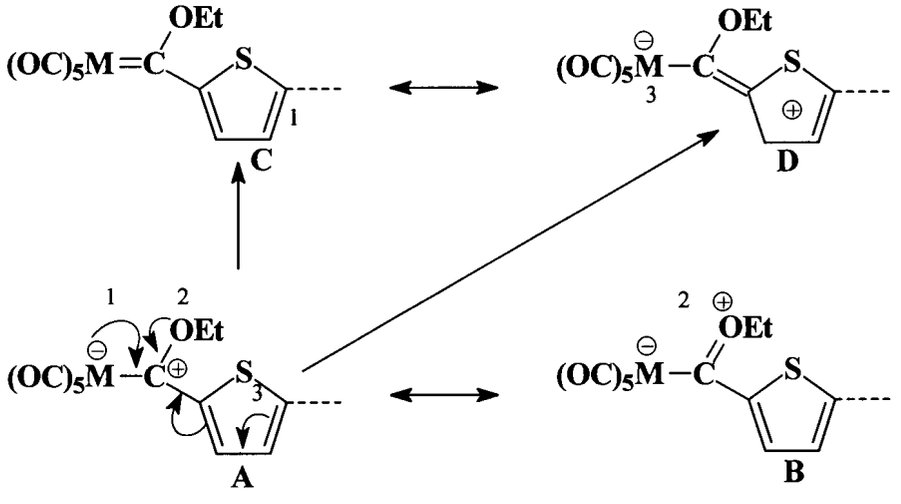

Figure 3.9 Charge delocalization on the carbene carbon

The canonical forms in figure 3.9 show a strong polarization towards the metal and towards the carbene carbon. The carbene carbon of **2** appears at 311.2 ppm, that of **3** at 301.9 ppm and that of **4** at 286.0 ppm. These values also show that "shielding of the carbon nucleus bonded to the metal atom increases with increasing atomic number of the metal"[4].

The signals of low intensity observed between 130 and 160 ppm are assigned to quaternary carbons (C2, C5, C6, C9 and C10) as shown in figure 3.7 for complexes **2-4**. Of these, only C2 can be assigned unambiguously as it is adjacent to the carbene carbon and therefore observed furthest downfield. The high intensity signals between 120 and 220 ppm are assigned to the carbons of the thiophene carbons with protons attached to them. They were assigned with the aid of the 2D HETCOR spectrum in figure 3.8.

The chemical shift of the methylene and methyl carbon atoms of the ethoxy group for **2-4** shows little variation. Both of them are shifted slightly downfield compared to resonances in ethanol. This is because the ethoxy group is bonded to an electrophilic carbene carbon which it stabilizes.

In the spectra of carbene complexes **2-4**, two signals were observed for the metal pentacarbonyl moiety. These signals are attributed to the *cis*- and *trans*-carbonyl carbons and have an intensity ratio of 1:4 (*trans*: *cis*) corresponding to the number of carbonyls in the complex. The carbonyl carbon signals for the three complexes lie in the region 203 to 224 ppm depending on the metal in the complex.

The general conclusion made is that the terthienyl ring is deshielded compared to uncoordinated terthienyl, which is indicative of charge transfer from the conjugated rings towards the carbene carbon.

3.3.1.3 INFRARED SPECROSCOPY

The infrared data for complexes **2-4** are summarized in table 3.4. Carbon stretching frequencies of the carbonyl region are represented by figure 3.10. It is evident from the data in table 3.4 that there is a substantial π-acceptor contribution of the carbene ligand.

Table 3.4 Carbonyl Stretching frequencies[a] of 2-4

BANDS	Stretching Vibrational Frequencies (cm^{-1})		
	2	3	4
$A_1^{(1)}$	2055	2065	2063
B	1980	1984	1971
$A_1^{(2)}$	1954	1942[b]	1948
E	1945	1942[b]	1935

[a]Solvent: Hexane [b]Signal overlap

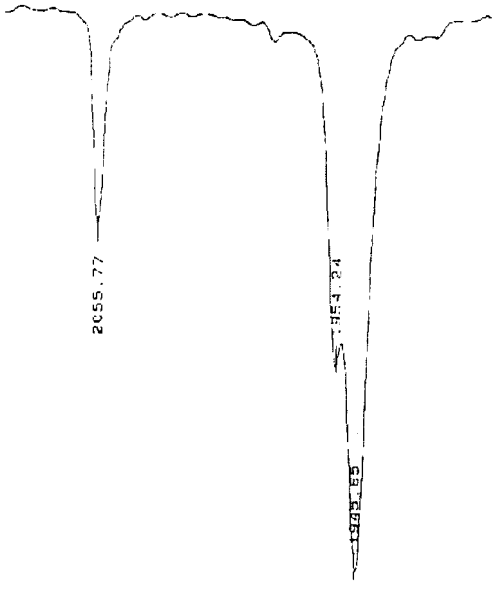

Figure 3.10 Spectrum of carbonyl stretching regions of complex 2

From the representative infrared spectrum (**2**) of complexes **2-4**, four absorption bands are distinguished in the terminal carbonyl region. Because the carbene carbon has a bulky substituent (terthienyl), the formally forbidden B-band is observed due to the distortion of the equatorial plane of carbonyls.

A strong carbonyl vibration absorption $A_1^{(2)}$ appears at the high frequency side of the E-band. This CO vibration is strongly affected by the *trans* ligand and its position is characteristic for the bonding properties of carbene ligands. For **3**, $A_1^{(2)}$ and E bands overlap resulting in an unresolved peak.

Lots of similarities exist between the carbonyl stretching frequencies in the thiophene carbene complexes[12] and the terthienyl monocarbene complexes **2-4**. This implied that an increase in the number of thiophene rings does not significantly affect the stretching vibrations of the carbonyl ligands.

3.3.1.4 Mass Spectrometry

Mass spectral data of the complexes **2-4** are tabulated in table 3.5. The three complexes showed the molecular ion (M^+) peak. The intensity of the M^+ ions of complexes **2-4** are very low. For complex **2**, the M^+ peak appears at m/z = 496, for **3** at 539 and for **4** at 627 respectively. First mode of fragmentation shows the stepwise cleavage of the metal – carbonyl ligand. A fragmentation route is presented in scheme 3.2.

For complex **2** and **4** the principle ion corresponds to the fragment M^+ -5CO whereas for complex **3** the principle ion corresponds to $HTTTH^+$. Complex **3** is not stable in the mass spectrometer and it is not possible to assign its fragments as easily as for **2** and **4**. The fragments corresponding to M^+, M^+ -5CO and $HTTTH^+$ are observed on this spectrum.

Table 3.5 Fragmentation data of complexes 2-4

Complex	Fragment ions (I, %)
2	496 (11) M^+; 468 (6) M^+ -CO; 412 (8) M^+ -3CO; 384 (20) M^+ -4CO; 356 (100) M^+ -5CO; 299 (38) M^+ -(5CO-COEt / Cr^+ -TTTH); 248 (7) $HTTTH^+$
3	539 (3) M^+; 399 (5) M^+ -5CO; 248 (100) HTTTH
4	627 (42) M^+; 599 (13) M^+ - CO; 571 (75) M^+ -2CO; 515 (58) M^+ - 4CO; 487 (100) M^+ -5CO; 248 (41) HTTTH

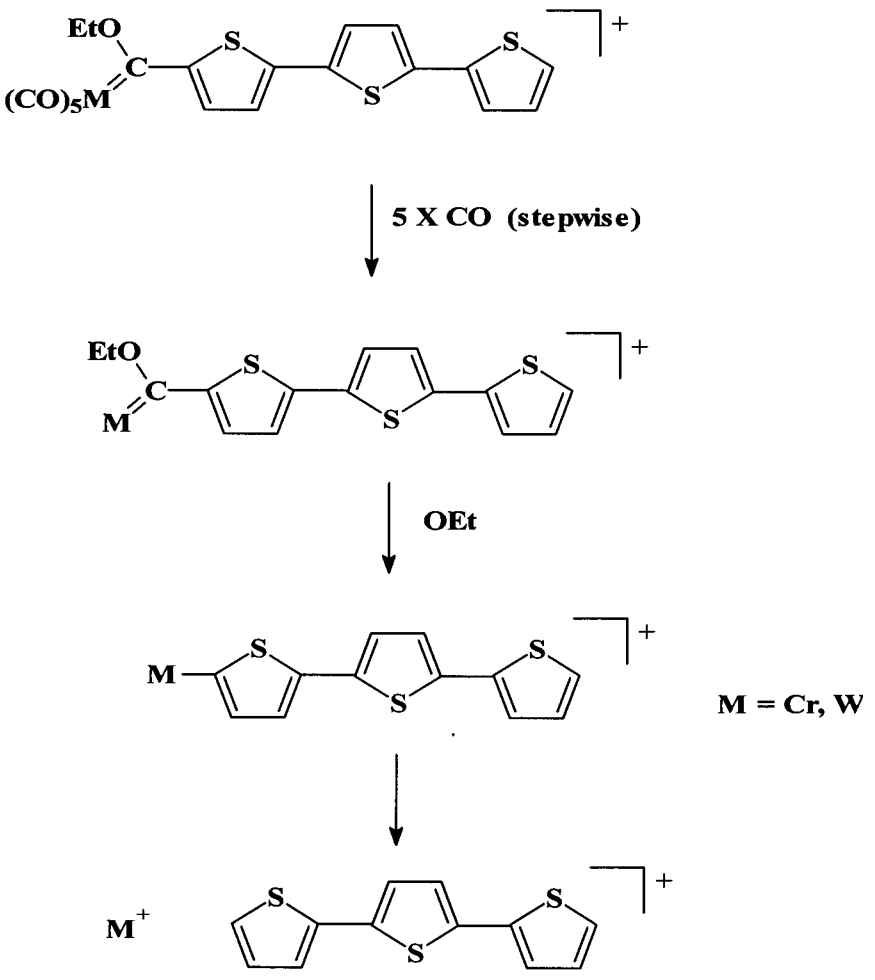

Scheme 3.2 Fragmentation patterns for complexes 2-4

3.3.1.5 Crystallography

Due to the poor quality of the crystals of complex 2, refining of the geometry was unsuccessful. Hence the bond angles and the bond lengths are not included in the structural analysis of complex 2. The crystal structure of complex 2 is shown in figure 5.2 of chapter 5.

3.4 Biscarbene Complexes

3.4.1 Characterization

3.4.1.1 ^{1}H NMR spectroscopy

^{1}H NMR data of complexes **5-7** are summarized in table 3.6. The ^{1}H NMR spectrum of complex **6** in figure 3.12 is used as a representative example of the complexes **5-7**.

Table 3.6 ^{1}H NMR data[a] of complexes 5-7

Protons	**5**		**6**		**7**	
	δ(ppm)	J(Hz)	δ(ppm)	J(Hz)	δ(ppm)	J(Hz)
H7,H7'	**7.35(s)**	-	**7.36(s)**	-	**7.37(s)**	-
H4,H4'	**7.32(d)**	**4.4**	**7.33(d)**	**4.4**	**7.32(d)**	**4.4**
H3,H3'	**8.17(d)**	**4.4**	**8.12(d)**	**4.4**	**8.08(d)**	**4.4**
CH_2 CH_3	**5.16(q)**	**7.05**	**5.04(q)**	**6.96**	**4.96(q)**	**6.96**
CH_2**CH_3**	**1.67(t)**	**7.05**	**1.65(t)**	**6.96**	**1.65(t)**	**7.23**

[a]Solvent : deuterated chloroform

Due to the symmetry of complexes **5-7,** the spectrum exhibits only three sets of signals in the aromatic region. The atom numberings in figure 3.11 are followed when assigning the protons to their respective resonances.

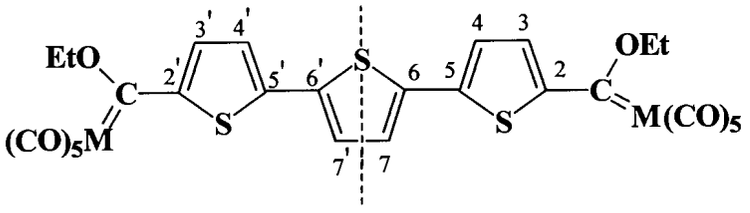

Figure 3.11 Atom numbering of biscarbene complexes 5-7

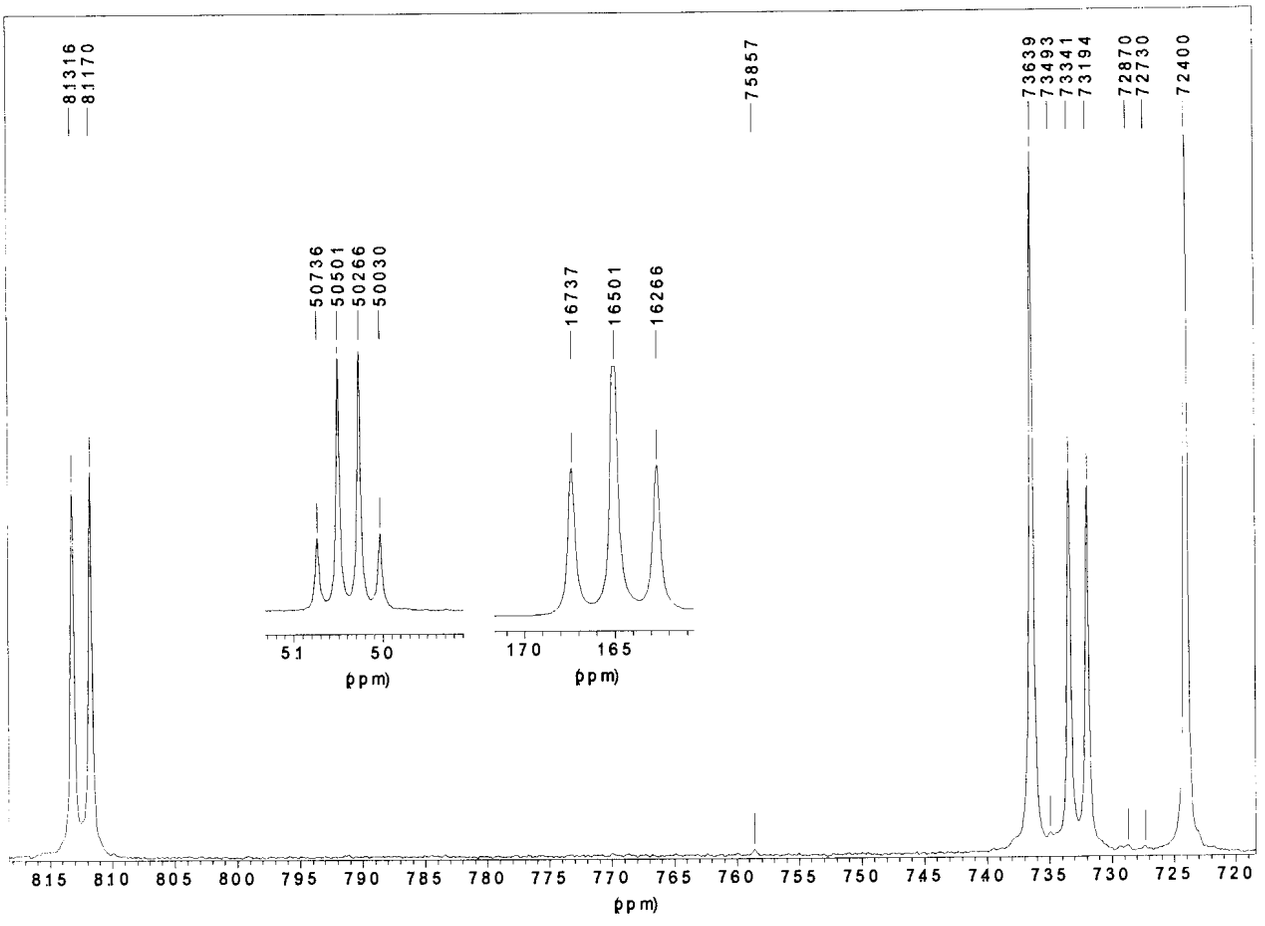

Figure 3.12 ^{1}H NMR spectrum of complex 6

The signal (d) that resonated far downfield between 8.08 ppm and 8.17 ppm for the three complexes is assigned to H3 because it is strongly deshielded by the electron withdrawing carbene carbon. The canonical forms in figure 3.9 still apply in explaining the deshielding of the aromatic protons, especially H3. Similar to the monocarbene complexes (**2-4**), deshielding of the protons depends on the increase in the atomic number of the metal. For H3, the trend is (Cr)>(Mo)>(W). There is a singlet which appears in the region 7.35 to 7.37 ppm for complexes **5-7**. This singlet is assigned to the protons H7 as shown in figure 3.12 because of the plane of symmetry bisecting the central thiophene ring. The doublet appearing in the region 7.32 to 7.33 ppm is assigned to H4.

Like free terthienyl, the three biscarbene complexes are symmetric. The only big difference between terthienyl and the three biscarbenes is the chemical shift position of the protons. The canonical forms in figure 3.13 illustrate the draining of electron density by the carbene moieties and metal fragments.

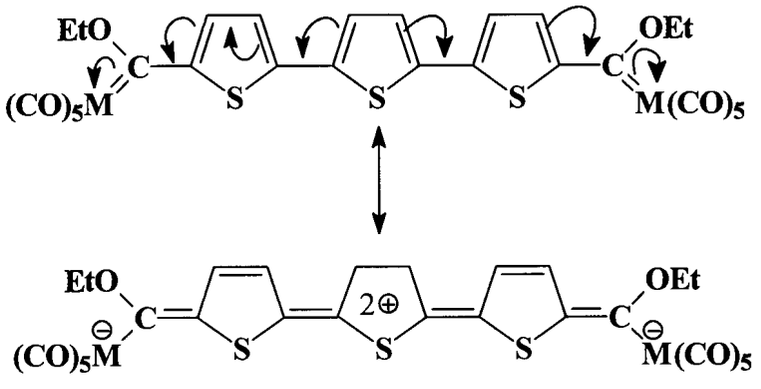

Figure 3.13 Electron delocalization in complexes 5-7

It can be seen from figure 3.13 that there is a strong polarization towards the metal and that proton H7 is slightly more deshielded than H4 but not nearly as much as the closer lying protons . This is explained by the positive charge on the central thiophene ring of the ligand. Figure 3.13 also shows that there is a draining of elecron density from both ends by the metal fragments which will affect the central thiophene more. In this respect figure 3.13 is exaggerated.

The methylene and methyl protons of the alkoxy substituents resonated at similar chemical shift values as those of the respective monocarbene complexes. The methylene protons resonate between 5.04 and 5.16 ppm and the methyl protons in the region 1.65 to 1.67 ppm. These chemical shift values confirmed the formation of the carbene complexes as they are characteristic for ethoxy carbene complexes of group 6 transition metals. The COSY spectrum of complex **7** in figure 3.14 is used as a representative example for the three biscarbene complexes **5-7**. From the COSY spectrum, one can see that proton H3 couples to H4.

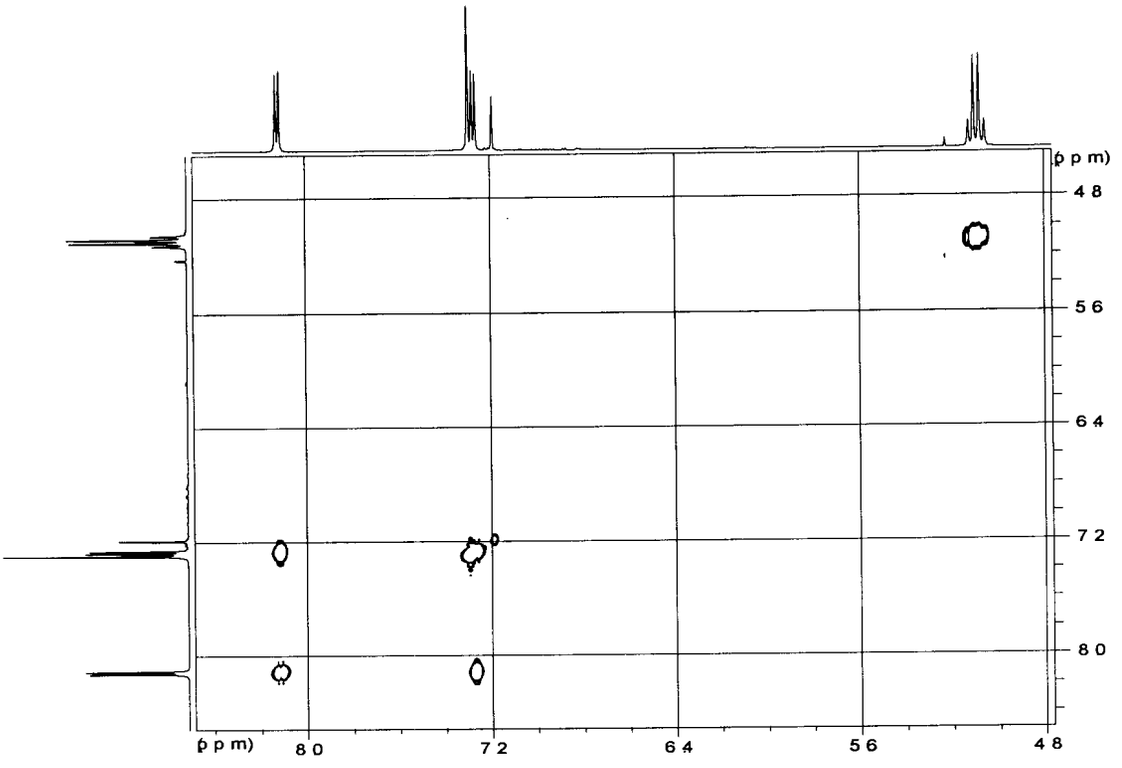

Figure 3.14 COSY spectrum of complex 7

3.4.1.2 ^{13}C NMR spectroscopy

The ^{13}C NMR data are summarized in table 3.7. The ^{13}C NMR spectrum of complex **6** in figure 3.15 is used as a representative spectrum for the three biscarbene complexes **5-7**. Deuterated chloroform was used as a solvent for NMR analysis.

Table 3.7 ^{13}C NMR data[a] of complexes 5- 7

Assignment Carbons	COMPLEXES Chemical Shifts (δ, ppm)		
	5	**6**	**7**
C1	312.5	303.2	287.6
CO(trans)	223.3	212.8	203.2
CO(cis)	217.1	206.1	198.2
C2	152.8	153.7	156.7
C5/6	145.3	146.2	146.9
C3	142.5	143.3	144.1
C5/6	137.8	138.0	138.7
C7	127.3	127.5	128.2
C4	125.7	125.7	126.3
$O\mathbf{CH_2}CH_3$	75.8	77.5	78.9
$OCH_2\mathbf{CH_3}$	15.2	15.1	15.71

[a]Solvent: deuterated chloroform

The aromatic part of the ^{13}C NMR spectrum of the biscarbene complexes **5-7** is shown in figure 3.15 and shows twelve carbons. Because complexes **5-7** have a plane of symmetry only six signals are observed for the aromatic part of the complex. Three quaternary carbon signals (signals with low intensity) appear between 130 and 160 ppm. These signals are assigned to carbons C2, C6, and C5 depending on the shielding they experience. Of these, C2 which is adjacent to the carbene carbon will be shifted furthest downfield.

The carbon C3 appears downfield from C4 and C7 because it is closer to the electrophilic carbene carbon and hence the most strongly deshielded of the three. In the region between 200 and 240 ppm two signals are observed, one of low intensity. The

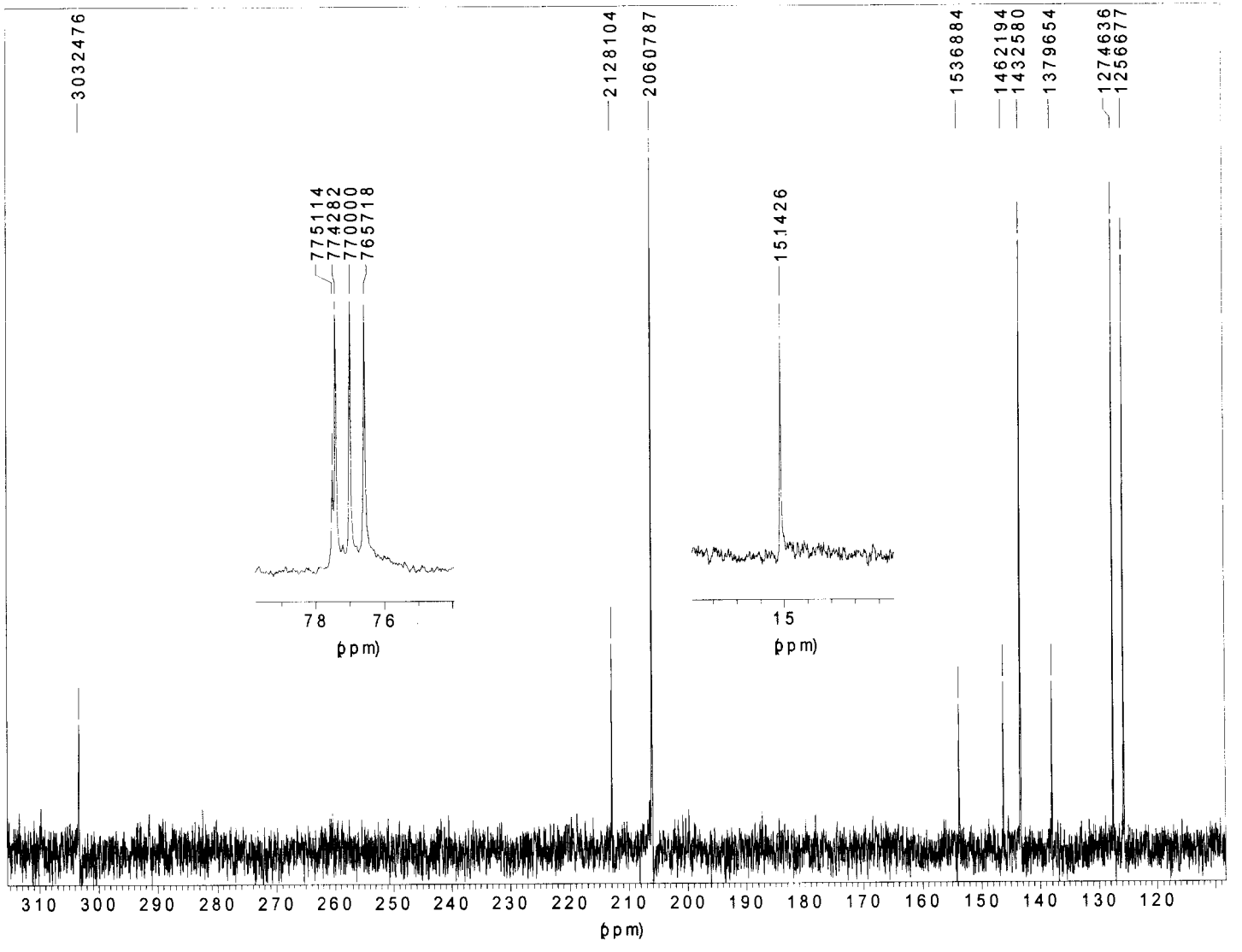

Figure 3.15 ^{13}C NMR spectrum of complex 6

signal of low intensity is assigned to the *trans* carbonyl while the one with higher intensity is due to the integration of the four carbons compared to one and is assigned to the *cis* carbonyl. The carbene carbon of the biscarbene complexes resonated further downfield compared to that of the monocarbene complexes but with small chemical shift differences. This can be attributed to the electron draining effect of biscarbenes from both ends.

Carbons were assigned with the aid of the HETCOR spectrum in figure 3.16.

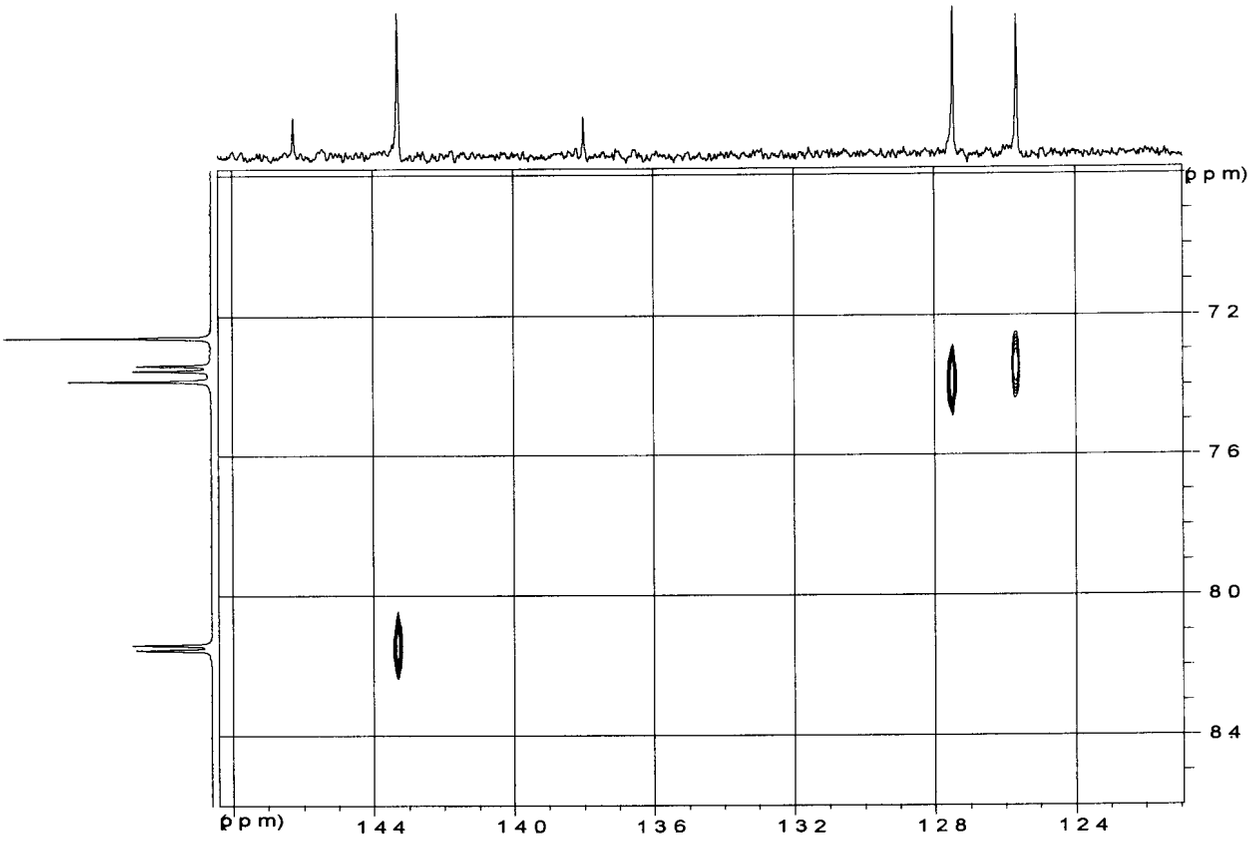

Figure 3.16 HETCOR spectrum of 5

3.4.1.3 Infrared spectroscopy

The infrared data of complex **5-7** are summarized in table 3.8 while the spectrum is depicted in figure 3.17.

Table 3.8 Infrared data[a] of complexes 5-7

BANDS	Stretching Vibrational Frequencies		
	5	7	6
$A_1^{(1)}$	2054	2062	2064
B	1983	1978	1985
$A_1^{(2)}$	1952	1952	1943[b]
E	1940	1945	1943[b]

[a]Solvent: Hexane [b]Signal overlap

For the biscarbene complexes (**5-7**), as was observed for the monocarbene complexes (**2-4**), the $A_1^{(2)}$ band is resolved and appears on the left of the E-band as depicted by figure 4.7. The formally IR-forbidden B band is clearly observed compared to the spectrum of complexes **5-7**.

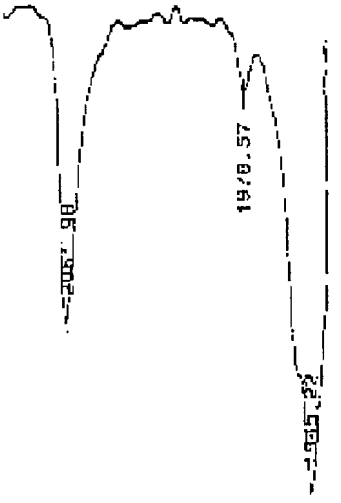

Figure 3.17 IR representative spectrum (7) of the complexes 5-7

3.4.1.4 Mass spectrometry

The M^+ signal was not observed for the three biscarbene complexes (**5-7**) and very few fragment ions displaying the transition metal isotope pattern could be assigned.

3.4.1.5 Crystallography

The final conformation of the structure of complex **7** was obtained from a single crystal X-ray diffraction study. The complex was crystallized from a 1:2 dichloromethane : hexane solution by using the layering technique at low temperature and under an inert atmosphere. Purple needle like crystals were obtained. The ball and stick representation of complex **7** is given in figure 3.18 with the labeling scheme used. The most important bond lengths and angles are listed in table 3.9. Complex **7** crystallized in the space group C2/c.

Table 3.9 Selected bond lengths and angles of complex 7

7	Bond Lengths (Å)	7	Angles (°)
W (1) - C (1)	2.225 (5)	C (12) -W (1) - C (1)	176.1 (2)
C (1) - C (2)	1.453 (6)	C (14) - W (1) - C (1)	93.56 (18)
C (5) - C (6)	1.455 (6)	C (11) - W (1) - C (1)	87.33 (17)
C (2) - C (3)	1.393 (6)	C (10) - W (1) - C (1)	91.03 (18)
C (4) - C (5)	1.391 (6)	C (13) - W (1) - C (1)	98.72 (17)
C (6) - C (7)	1.406 (6)	O (1) - C (1) - W (1)	129.6 (3)
C (3) - C (4)	1.417 (6)	C (1) - C (2) - C (3)	128.7 (4)
C (7) - C (7A)	1.417 (6)	C (4) – C (5) - C (6)	125.8 (4)
S (1) - C (2)	1.760 (4)	C (7) – C (6) - C (5)	130.8 (4)
S (1) - C (5)	1.728 (4)	C (1) – C (2) - S (1)	121.4 (3)
S (2) - C(6)	1.727 (4)	C (6) – C (5) - S (1)	123.3 (3)
S (2) - C (6A)	1.727 (4)	C (2) – C (1) - O (1)	106.4 (4)
O (1) - C (1)	1.344 (5)	C (2) – C (1) - W (1)	124.3 (4)
O (4) - C (12)	1.140 (6)		
O (5) - C (13)	1.139 (6)		
W (1) - CO (cis)	2.027 (6) average		
W (1) - CO (trans)	2.049 (5)		

In Fischer carbene complexes, it is well known that the heteroatom (X = N, O and S) stabilizes the carbene complex by its electron pair donation to the carbene carbon atom. The resulting partial double bond character between the heteroatom and the carbene carbon is indicated by the shortening of the carbon heteroatom bond C-X.

The $W(CO)_5$ fragments are *trans* to the sulfur atoms of the terthienyl spacer which places them on the same side of the molecule. This was also observed for $(CO)_5CrC(OEt)TC(OEt)Cr(CO)_5$ and represents the energetically favoured position for an uneven number of thienyl rings in the spacer moiety. The bond lengths of W(1) - C(1) is the longest reported for tungsten carbene complexes but still falls within the range reported for alkoxy carbene complexes of tungsten[12]. This is because the $W(CO)_5$ fragment is competing with both the ethoxy group and the conjugated ligand to stabilize the electrophilic carbene carbon. The less the M-C π interaction the longer the bond. Draining of the electron density from the terthienyl substituent and π lone pair donation from the ethoxy group reduces back-bonding from the metal thereby lengthening the W-C(1) bond. The $W\text{-}C_{carbonyl}$ and C-O bond lengths are as expected i.e. the $W\text{-}C_{carbonyl}$ is shorter and the C-O bond longer as a result of the σ-donor and π-acceptor characteristics of the carbonyl carbon in the ligand ($C{\equiv}O$ vs $M{=}C{=}O$).

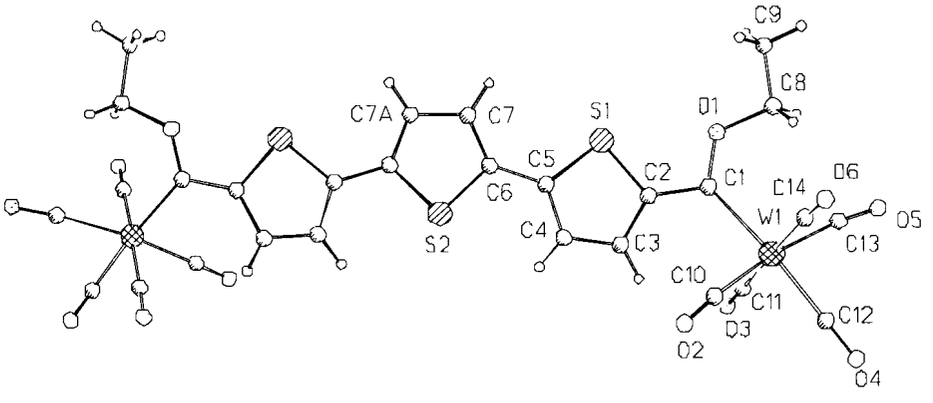

Figure 3.18 Ball and stick plot of W

[12] (a) K.H. Dötz, H. Fischer, P. Hofmann, F.R. Kreissl, U. Schubert, K. Weis, "Transition Metal Carbene Complexes", Verlag Chemie GmbH, Weinheim,1983.

(b) Y.M. Terblans, H.M. Roos, S. Lotz, J.Organomet.Chem.,1998,566,133.

The $M(CO)_5$ fragment is slightly distorted (124.3°) and bent away from the terthienyl substituent. The greatest distortion on the $M(CO)_5$ is obtained for C(13) – W(1) – C(1) (98.72°).

In our structure there are three thiophene rings and the structural study indicates that the dihedral angle between S(1) – C(5) – C(6) – S(2) is 178.0° anti-clockwise which indicates that the thiophene rings of complex **7** are flat and facilitates the distribution of π-delocalization.

Structural data for the dihedral angle between W – C – C – S indicates rigidity around the C – C single bond. From this one can conclude that the thiophene rings can be orientated parallel to the M – C – double bond for the dihedral angle 0 or 180°. The value obtained for the dihedral angle between W(1) – C(1) – C(2) – S(1) is 166.2°.

The bond lengths of the *trans* W – (CO) are slightly longer than the average value for the four *cis* W – (CO) distances. This shows the poorer π-acceptor properties of the carbene ligand compared to the carbonyl ligand (the carbenes have only one p-orbital for acceptance while the carbonyls have two perpendicular antibonding orbitals).

The average bond length between a double bond, $sp^2(C) = O(sp^2)$, is shorter than the C(1) – O(1) bond length and C(1) – O (1) is shorter than a $sp^2(C) – O(sp^3)$ single bond. This indicates the partial double bond character between the $sp^2(C) – O(sp^2)$.

3.4.1.6 UV spectroscopy of both mono and biscarbene complexes (2-7)

Generally carbene complexes show a remarkable variation in colour. All the carbene complexes (2-7) are coloured because they absorb broad bands of visible radiation in at least one of their oxidation states. Absorption involves transition of electrons between filled and unfilled d-orbitals of chromium, tungsten and molybdenum with energies that depend

on the nature of the ligand bonded to them. From this we can say that the position of absorption peaks depend on the position of the element in the periodic table, its oxidation state and the nature of the ligand bonded to it. The UV data of the complexes are summarized in table 3.10.

Table 3.10 UV data[a] of complexes 2-7

Complex	Colour	Ligand π-π* - transitions	Metal-Ligand transitions	Ligand based absorptions
2	Red	418.0	514.0	253.0
3	Red	352.4	529.0	256.0
4	Red	352.5	544.0	256.0
5	Purple	418.0	556-565	253.0
6	Purple	415.0	532-559	253.0
7	Purple	406.0	559.0	253.0

[a]UV-peak wavelengths are reported in nanometers (nm).

The electronic spectra of monocarbene complexes (**2-4**) are shown in figure 3.19 and that of the biscarbene complexes (**5-7**) in figure 3.20. The highest wavelength absorption band in the electronic spectra in figure 3.19 which had undergone a bathochromic shift due to the heteroatom of the stabilizing group can be assigned to a π-π* transitions[13].

[13] E.O.Fischer, Pure.Appl.Chem., 1970, 24, 407.

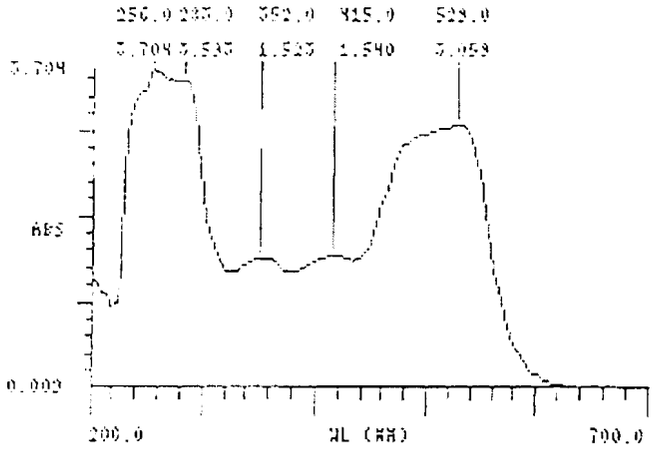

Figure 3.19 UV-spectra of complex 3

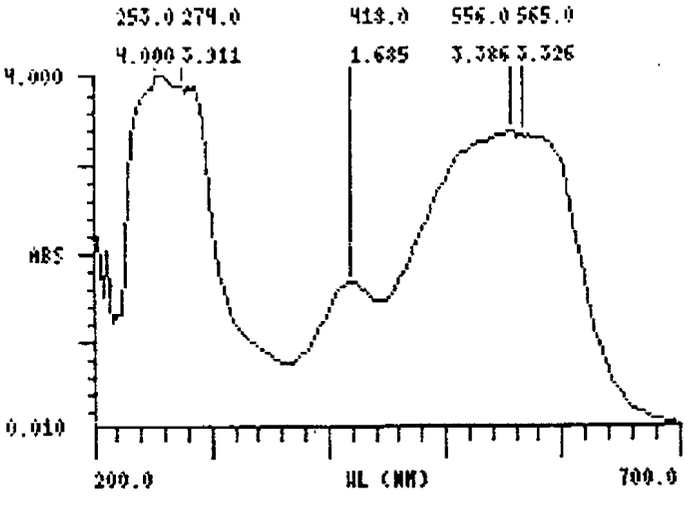

Figure 3.20 UV-spectrum of complexes 7

Less intense absorption bands with λ-maximum in the range 220 to 460 nm are assigned to the terthienyl based transitions. These bands are more intense in the spectrum of free terthienyl. From the spectra, one can see that on metallating terthienyl, the interband transitions decrease and the absorption peak shifts towards higher energy. A series of absorption bands of high intensity appear between 530 and 570 nm for biscarbene complexes and 510 to 550 nm for the monocarbene complexes respectively. These results support the conclusion that the π-system of conjugated oligothienyl ligands interacts with the carbene carbon and terminal metals.
Monocarbene complexes are represented by the spectrum of complex **3**. The biscarbene complexes (**5-7**) are represented by the spectrum of **7** in figure 3.20.

3.4.1.7 Conclusion

Monocarbene complexes were obtained as byproducts of the synthesis of biscarbene complexes. Reddish-brown products were obtained compared to the purple colour of the biscarbene complexes. This is ascribed to the incomplete double lithiation during the metallation step. The mono and biscarbene complexes are remarkably stable and no decomposition products were observed. The complexes were characterised by NMR spectroscopy and the structure of the biscarbene confirmed by a single crystal structure determination of the W analogue. Spectroscopic data revealed that monocarbene complexes are not planar/flat like the biscarbene complexes. Through spectroscopic data, it was found that biscarbene complexes allow metal-metal communication through the spacer ligand as illustrated in the figure below. Also, in the solid state the terthienyl is flat and in conjugated plane with the carbene carbons and metals.

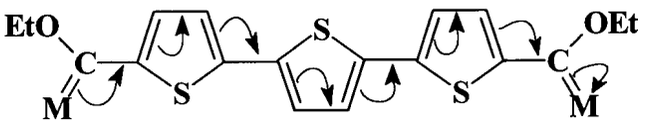

Figure 3.21 Metal communication in spacer for biscarbene complexes

CHAPTER 4

AMINOCARBENE COMPLEXES

4.1 General introduction

Carbene complexes with an alkoxy group can be regarded as esters in which the ketonic oxygen atom has been substituted by a $M(CO)_5$ group (M= Cr, W, Mo). The reactivity of group 6 transition metal Fischer carbene complexes has been exploited in a wide variety of thermal and photochemical synthetic methodologies, thus making it to reach a very large number of versatile organic and organometallic targets (also stereoselective)[1].

The carbene carbon atom of the alkoxycarbene complexes show a remarkable susceptibility to nucleophilic attack. Exchange processes involving the displacement of the alkoxy group from the alkoxy carbene complexes by amines normally prepare aminocarbene complexes, although the route is limited to the use of sterically unhindered amines[2]. The reaction involves the elimination of the alcohol and the formation of the aminocarbene product as illustrated by figure 4.1.

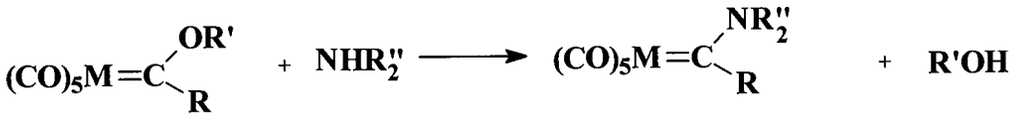

Figure 4.1 Aminolysis reaction of alkoxy carbene complexes

---

[1] S.Maiorana, E.Licandro, L.Capella, D.Perdichia, A.Papagni, Pure. Appl.Chem., 1999, 78, 1453.

[2] (a) U.Klabunde, E.O.Fischer, J.Am.Chem.Soc., 1967, 89, 7141.

(b) J.A.Connor, E.O.Fischer, J.Chem.Soc.A., 1969, 578.

(c) E.Moser, E.O.Fischer, J.Organomet.Chem., 1969, 16, 275.

(d) E.O.Fischer, B.Heckl, H.Werner, J.Organomet.Chem., 1971, 28, 359.

(e) P.E.Baikie, E.O.Fischer, O.S.Mills, J.Chem.Soc.Chem.Comm., 1967,1199.

(f) F.R.Kreissl, In Transition Metal Carbene Complexes, Syferth, D., Ed., Verlag Chemie: Deerfield Beach, FL, 1983.

Aminocarbene complexes slightly differ from the alkoxy carbene complexes because of greater donation of the heteroatom lone pair to the carbene carbon. Double carbon-nitrogen bond is an acceptance structure as presented by figure 4.2. Thus the nitrogen atom is more involved to stabilize the electrophillic carbene carbon. The aminocarbene chemistry of chromium has been studied extensively. From these studies, restricted rotation around the C-N bond originating from the π donation from the nitrogen atom affords geometric isomers. The negative charge on the metal fragment is redistributed to the carbonyl ligands.

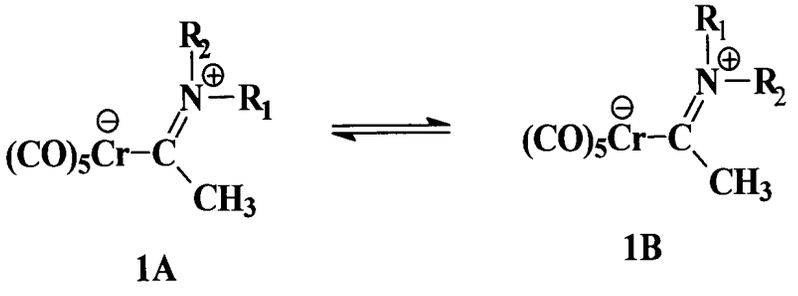

Figure 4.2 Rotamers 1A and 1B of aminocarbene complexes

When R_1 and R_2 are different, two different stable Z and E isomers are generated and usually equilibrate under basic reaction conditions[1a] as shown in figure 4.2

A series of C_2 symmetric amines were synthesized by Maiorano *et al.*[1] as shown by the reaction scheme in figure 4.3

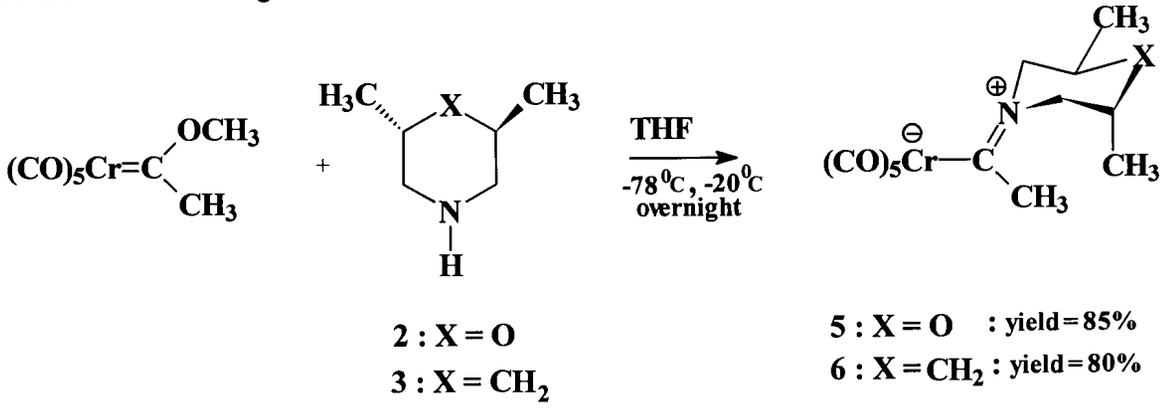

Figure 4.3 Reaction scheme of C_2 symmetric amines

Interesting results were obtained from this reaction. It was found that these complexes exist in solution, as well as in solid state as a single rotamer. According to Maiorano the anions of Fischer aminocarbenes could be good candidates in reactions with nitrolefins, since they are soft nucleophiles and have proved to be reactive with a variety of electrophiles under very mild conditions. The aminolysis of methoxylphenylcarbene(pentacarbonyl)chromium has been studied in detail and appears to involve a complicated reaction[3]. Recently in our laboratory ethoxy(thienyl)carbene(pentacarbonyl)molybdenium was synthesized[4] and studied. The proton NMR spectrum displayed two broad peaks which were characteristic of the NH_2 group. It was found that the Z-proton appears more downfield than the E-proton as was reported by N.Hoa Tran Huy[5].

A very efficient and relatively general method for the preparation of chromium aminocarbene complexes was recently reported by Imwinkelried and Hegedus[6] as illustrated in figure 4.4.

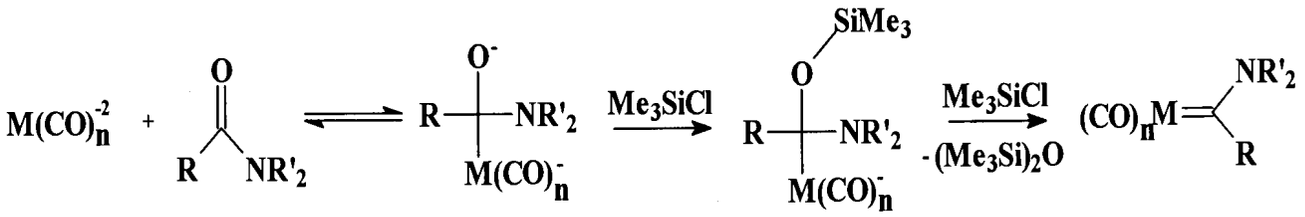

Figure 4.4 Synthesis of aminocarbene complexes

[3] (a) B.Heckl, H.Werner, E.O.Fischer, Angew.Chem.Int.Ed.Engl., 1968, 7, 817.
(b) H.Werner, E.O.Fischer, B.Heckl, C.G.Kreiter, J.Organomet.Chem., 1971, 28, 367.

[4] M.Landman, Thesis "Synthesis of metal complexes with thiophene ligands", 2000, 42.

[5] N.Hoa Tran Huy, P.Lefloch, F.Robert, Y.Jeannin, J.Organomet.Chem., 1987, 327, 211.

[6] R.Imwinkelried, L.S.Hegedus, Organometallics, 1988, 7, 702.

The scope of the reaction in figure 4.4 has been explored using other substrates with the aim of preparing iron aminocarbene complexes bearing hydrogen, aromatic or heteroaromatic substituents at the carbene carbon atom. The longest bisaminocarbene complex to date with twelve carbon atoms in the chain (C_x) was reported by Fischer *et al.*[7]. Aminolysis and the introduction of amine groups of the centrosymmetric coplanar bimetallic bisphenylene biscarbene complexes gave the corresponding biscarbene complexes of tungsten and chromium in figure 4.5[5].

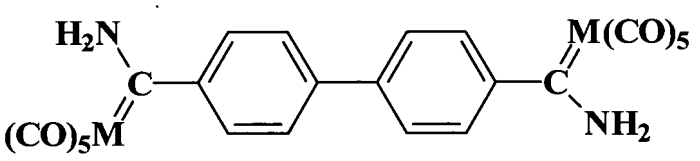

M = Cr
M = W

Figure 4.5 Bimetallic bisphenylene bisaminocarbene complexes

4.2 Synthesis of aminocarbene complexes

Aminocarbene complexes were prepared by bubbling gaseous ammonia through an ether solution[8] containing the carbene complexes **2**, **3**, **4** and **5**. An immediate colour change occurred. Upon removal of the solvent under reduced pressure pale yellow crystals were obtained representing the monoaminocarbene complexes **8** and **9**, and the orange coloured represented the bisaminocarbene complexes **10** and **11**. Complexes were purified by column chromatography under an inert atmosphere of nitrogen at low temperatures.

Based on full characterization it was concluded that the pale yellow products are monoaminocarbene complexes and the orange products are the bisaminocarbene complexes.

---

[7] C.Hartbaum, E.Mauz, G.Roth, K.Weissenbach, H.Fischer, Organometallics, 1999, 18, 2619.

[8] E.O.Fischer, A.Maasböl, Angew.Chem., Int.Ed.Engl, 1964, 3, 580.

4.3 Monoaminocarbene complexes

The reaction scheme for the aminolysis resulting in the products **8** and **9** is shown in figure 4. 6.

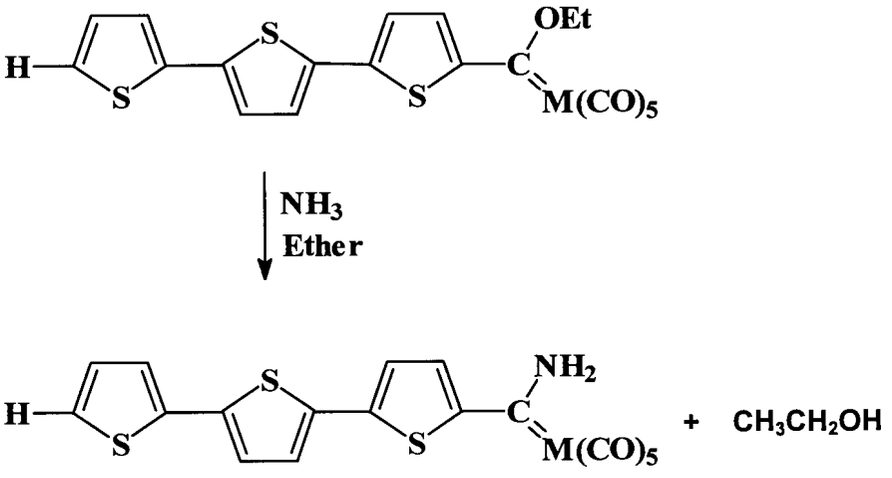

M= Cr (8)
M= W (9)

Figure 4.6 Reaction scheme for the formation of 8 and 9

4.3.1 Spectroscopic characterization

The complexes were characterized with NMR, IR, and UV spectroscopies and Mass spectrometry. Assignment of protons is based on the atom numbering in figure 3.4.

4.3.1.1 ^{1}H NMR spectroscopy

The ^{1}H NMR data of the complexes **8** and **9** are summarized in table 4.1. The complexes are represented by the spectrum of **9** in figure 4.7.

Table 4.1 **^{1}H NMR data[a] of 8 and 9**

Protons		**8**			**9**	
	δ(ppm)	J_3(Hz)	J_4(Hz)	δ(ppm)	J_3(Hz)	J_4(Hz)
H12	**7.12(2xd)**	**4.40, 4.40**	-	**7.12(2xd)**	**5.16, 3.63**	-
H11	**7.38(dd)**	**3.60**	**1.02**	**7.39(dd)**	**3.63**	**1.14**
H13	**7.50(dd)**	-	**1.29**	**7.50(dd)**	**5.16**	**0.96**
H3	**7.78(d)**	**4.11**	-	**7.77(d)**	**4.20**	-
H4	**7.51(d)**	**4.11**	-	**7.48(d)**	**4.20**	-
H7	**7.46(d)**	**3.87**		**7.46(d)**	**3.81**	-
H8	**7.31(d)**	**3.90**		**7.31(d)**	**3.81**	-
H-N-H[b]	**10.20**	-		**10.24**	-	
		-		**9.96**	-	

[a]Solvent: Deuterated acetone

[b]Broad signals with low intensity are obtained for the amino protons.

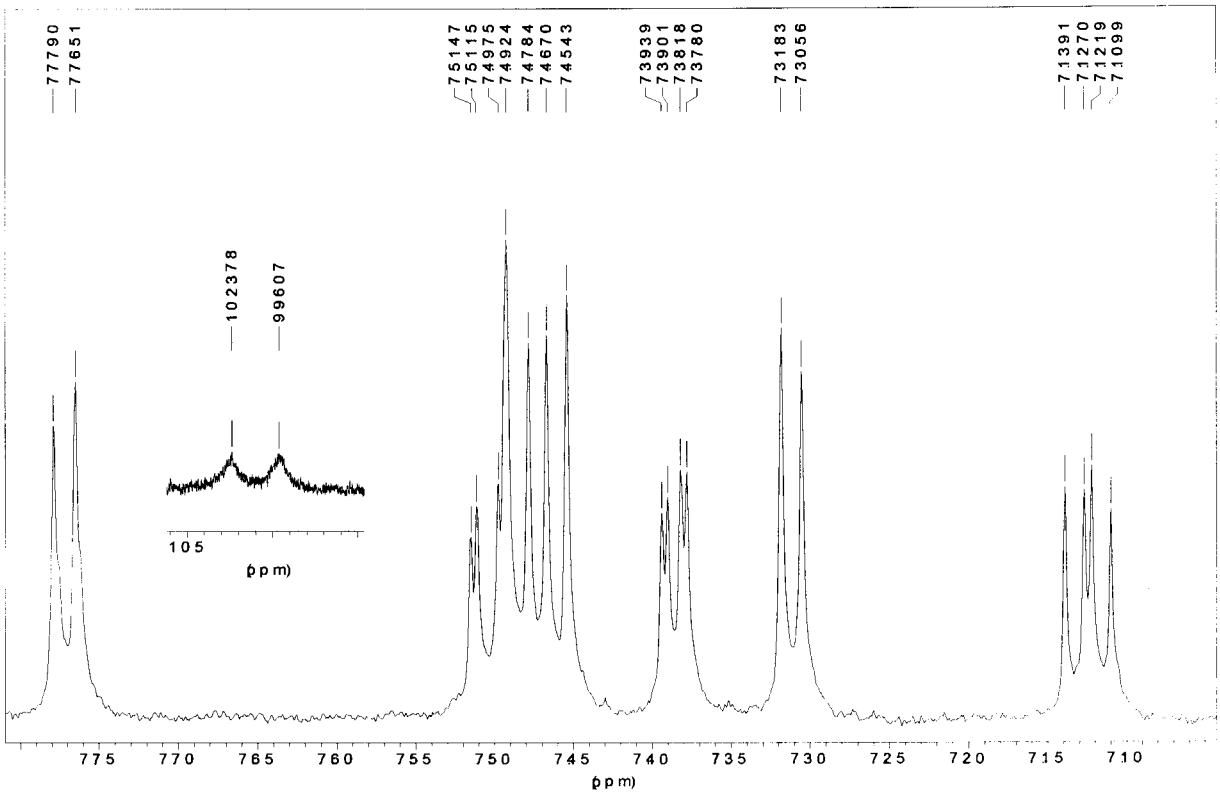

Figure 4.7 **^{1}H NMR spectrum of 9 in the thiophene region**

The data in table 4.1 support the proposed molecular structures of the two complexes **8** and **9**. The protons of the heteroaromatic part lies in the range 7.12 ppm to 7.8 ppm.

These show an enormous upfield chemical shift compared to those of the corresponding ethoxy(terthienyl)carbenepentacarbonylmetal complexes (**2** and **3**). It is evident that the NH_2 group plays a major stabilizing role. From the chemical shifts, it is evident that the NH_2 group is a stronger π-donor than the ethoxy group. Coupling constants were employed to assist in the assignment of the aromatic protons.

From the spectrum in figure 4.7, two broad signals are observed at 9.90 and 10.25 ppm. These signals are assigned to the protons of the amino group ($-NH_2$). They are broad due to the quadrapolar broadening. Due to the slow rate of nuclear spin states of nitrogen, these signals can clearly be observed.

For complex **8** only one broad signal is observed on the spectrum. This did not come as a surprise because the NH resonance is sometimes subjected to such a large broadening effect that it is difficult to distinguish the absorption from the baseline of the spectrum.

For complex **9**, two broad signals appear far downfield because the amino group is bonded to the electrophilic carbene carbon. This is also consistent with the double bond character of the carbene carbon-nitrogen bond and electropositive nitrogen atom.

The doublet at 7.78 and 7.77 ppm is assigned to H3 for complex **8** and **9** respectively. The downfield chemical shift is ascribed to the electron draining effect of the carbene moiety. The canonical forms used to explain the electron draining effect of the carbene carbon in chapter 3 in figure 3.5 still applies for aminocarbene complexes.

A doublet of doublets at 7.50 ppm for **9** and **8** is assigned to H13 because of conjugation and the deshielding effect of the heteroatoms it experiences. The doublet for H13 is not well resolved because of the doublet of H4.

Figure 4.2 also shows that conversion of protons H_Z and H_E takes place. Two signals were obtained for the amino protons because this transition does not take place very rapidly. Nitrogen has only a moderately sized quadrapolar. Assignment of the other signals (H4, H7, H8, H11, H12) in figure 4.8 is similar to that of the ethoxy carbene complexes **2-4**. The splitting patterns of the interacting nuclei H13, H12, H11 and H8 and H7, H4, H3 are shown in figure 4.7. The seven nuclei have different chemical shifts. Each nuclear signal is split by a three bond coupling with adjacent protons (J_3). H13 is split into a doublet of separation J_3 by H12 and further split into a doublet of separation J_4 by H11. The reverse order of couplings exists for H11 and in both cases we have doublet of doublets.

Coupling constants in these complexes also depend on the bond lengths and the charge distribution in the complex. Usually long range couplings J_4 are often less than 1 Hz, but since the bonds linking the coupled nuclei are in a sterically fixed configuration, the coupling constants are larger in our complexes, as shown in table 4.1.

Similarly to the ethoxycarbene complexes, complex **8** and **9** are dependent on the angle between the C-H bond and the axis of the double bond.

4.3.1.2 ^{13}C NMR spectroscopy

The ^{13}C NMR spectra of **8** and **9** could not be obtained due to the poor solubility of these complexes.

4.3.1.3 Infrared Spectroscopy

IR data of complexes **8** and **9** are presented in table 4.2.

Table 4.2 Infrared data[a] of 8 and 9

BANDS	Stretching Vibrational Frequencies(cm^{-1})	
	8	**9**
***V*(NH)**	2925 2854	2924 2853
$A_1^{(1)}$	2063	2063
B	1980	1969
$A_1^{(2)}$	1933	1926
E	1933	1926

[a]Solvent: Dichloromethane

Similar to the ethoxy carbene complexes, the metal carbonyl fragment of complex **8** and **9** displays C_{4v} symmetry and have the same vibrational classifications. The carbonyl stretching region of the IR spectra of the complexes **8** and **9** looks very similar. They all show a sharp band of medium intensity at 2063 cm^{-1} assigned to $A_1^{(1)}$, a weak band at 1969 cm^{-1} for **9** and 1980 cm^{-1} for **8** assigned to B and a broad very intense band at 1926 cm^{-1} for **9** and 1933 cm^{-1} for **8** assigned to E and $A_1^{(2)}$ which overlaps.

The NH_2 group showed two signals at 2855 cm^{-1} and 2926 cm^{-1}. These agree with the results obtained by Connor and Fischer[9] for amino carbene complexes of chromium. The stretching vibrations of **8** and **9** appear at lower wavenumbers compared to those reported for chromium aminocarbene complexes. They used a methyl substituent whereas we used terthienyl for the corresponding substituent. Terthienyl is a stronger electron donor compared to methyl substituent, thus lessening the electron contribution required from the NH_2 group to the carbene carbon. The effect of the electron withdrawing carbene carbon is somewhat smaller, probably due to increased electron donation from the NH_2 group. Structural evidence[10] led to the conclusion that amino substituents are better π-donors than ethoxy substituents. As a result, aminocarbene complexes display less metal to the carbene carbon π-back donation, hence an increase in backbonding from the metal to the carbonyl carbons is required. This effect results in higher M-$C_{carbonyl}$ bond orders and a decrease in the $C_{carbonyl}$-O bond order. The lower stretching frequencies observed in the spectra of complex **8** and **9** compared to those of ethoxy carbene complexes **2-7** confirm this observation.

4.3.1.4 Mass spectrometry

A strong molecular ion peak was observed in the spectrum of **8.** The initial fragmentation pattern is unclear, but fragments represent the stepwise fragmentation of carbonyls. A summary of the most important fragmentation peaks is given in table 4.3. The most intense peak found at m/z = 459 which correlates with the loss of the five carbonyl ligands and HCN from the parent molecule. For complex **9**, the molecular ion peak M^+ was not observed and very few fragment ions displaying the transition metal isotope pattern could be assigned.

---

[9] J.A.Connor, E.O.Fischer, J.Chem.Soc., 1969, A, 578.

[10] (a) M.Y.Darensberg, D.J.Darensberg, Inorg.Chem., 1970, 9, 32.

(b) J.A.Connor, J.P.Lloyd, Chem.Rev., 1970, 3237.

Table 4.3 Mass spectral data for 8

Complex	Fragment ions (m/z)
8	598 (23) M^+; 543 (15) M^+ - HCN-CO; 515 (15) M^+ -HCN-2CO; 459 (100) M^+ -HCN-4CO; 248 (77) $HTTTH^+$.

4.4 Bisaminocarbene Complexes

Reaction mechanism for aminolysis of biscarbene complexes **10** and **11** is shown in figure 4.8.

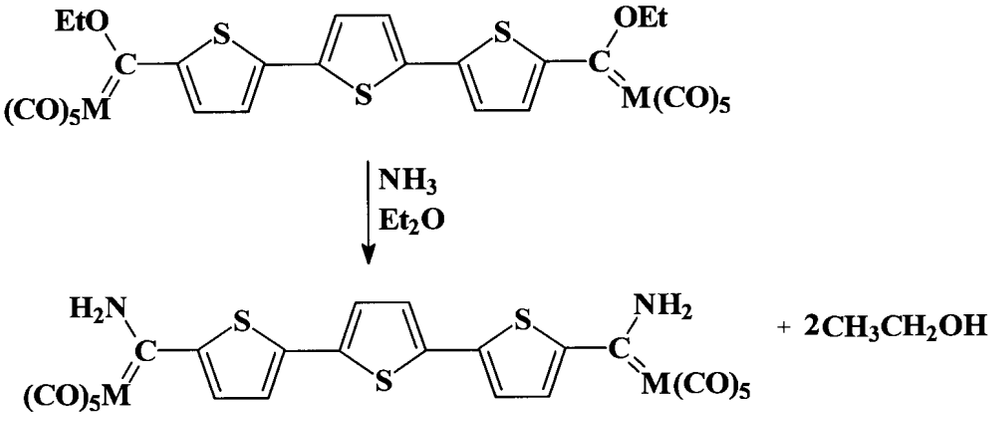

M=W -10
=Cr-11

Figure 4.8 Reaction scheme of 10 and 11

4.4.1 Characterization

The bisaminocarbene complexes were characterized by NMR and IR spectroscopy. The spectroscopic data are in accordance with their formulation.

4.4.1.1 ^{1}H NMR Spectroscopy

The ^{1}H NMR data of **10** and **11** are summarized in table 4.4. The ^{1}H NMR spectrum of complex **11** in figure 4.9 is a representative example of the bisaminocarbene complexes.

Table 4.4 **^{1}H NMR data[a] of 10 and 11**

Protons	10		11	
	δ(ppm)	J(Hz)	δ(ppm)	J(Hz)
H4, H4'	**7.78(d)**	**4.14**	**7.73(d)**	**3.99**
H3, H3'	**7.58(d)**	**4.14**	**7.52(d)**	**3.68**
H7, H7'	**7.53 s**		**7.51 s**	
H-N-H	**10.26**	**One broad signal**	**10.31 9.87**	**Two broad signals**

[a]Solvent: Deuterated acetone

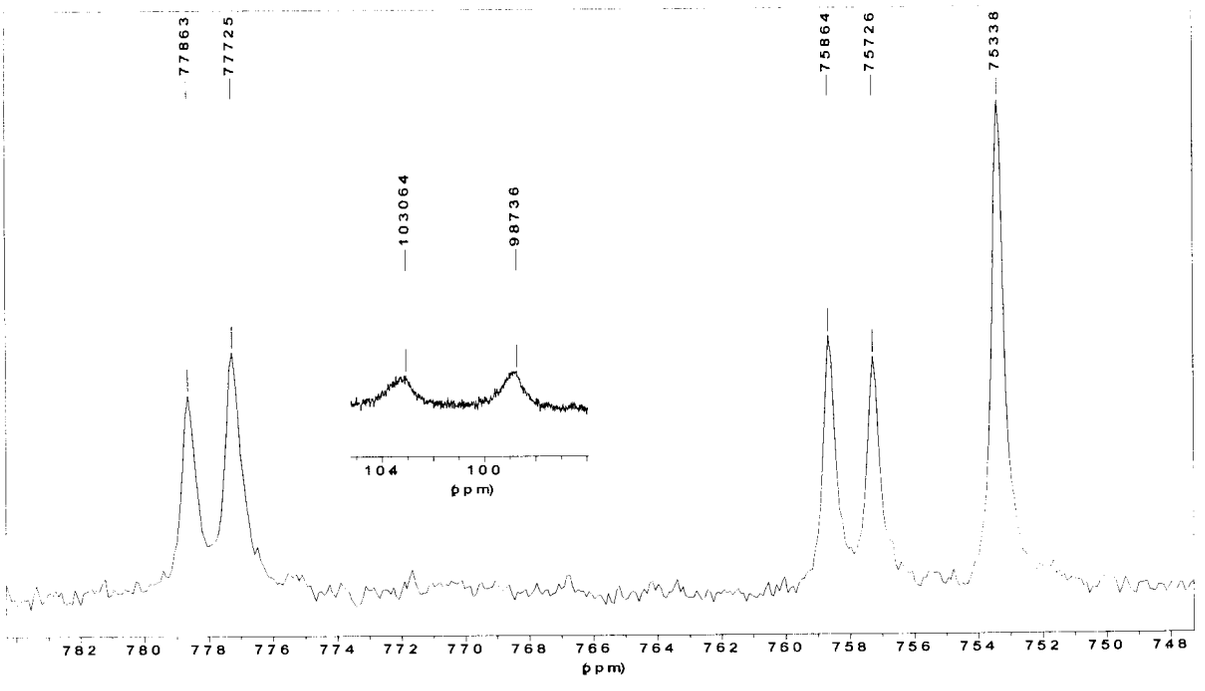

Figure 4.9 **^{1}H NMR spectrum of 11**

From the spectra in figure 4.9, two broad signals are observed at 9.87 and 10.30 ppm. Like in monoaminocarbenes, these signals are assigned to the protons of the amino group. This is due to the quadrapolar broadening as the nuclear spin states of nitrogen are slow.

In **10**, the upfield amino group signal is not observed because it is subjected to a broadening effect that makes it difficult to distinguish the absorption from the baseline. From the ^{1}H NMR data in table 4.4, it can be seen that shielding of protons and carbons increase with the increase in the atomic number of the metal in a group.

The downfield shift of the amino group protons is in accordance with electron donation from the nitrogen lone pair to the carbene carbon atom.
By just looking at the spectrum in figure 4.9, one can see that **10** and **11** have a plane of symmetry. The spectra of **10** and **11** exhibit two doublets of doublets and a singlet in the aromatic region. The doublet at 7.78 ppm is assigned to H3 because of the electron withdrawing effect of the carbene carbon moiety. The singlet at 7.53 ppm is assigned to H7 resulting from the plane of symmetry passing through the central thiophene unit.

The thiophene protons **10** and **11** are upfield compared to those of the respective ethoxy carbene complexes **5** and **6**.

4.4.1.2 ^{13}C NMR spectroscopy

Solutions of **10** and **11** could not be obtained sufficiently concentrated to measure and assign the ^{13}C NMR signals. The complexes formed a precipitate during ^{13}C NMR measurements and only the solvent signals were observed.

4.4.1.3 Infrared spectroscopy

Infrared data of **10** and **11** are summarized in table 4.5.

Table 4.5 IR data[a] of 10 and 11

BANDS	Stretching Vibrational Frequencies(cm^{-1})	
	10	**11**
***V*(NH)**	2926 2854	2988 2979
$A_1^{(1)}$	2062	2054
B	1968	1968
$A_2^{(2)}$	1923	1930
E	1923	1930

[a]Solvent: Dichloromethane

The C-O stretching frequencies of metal carbonyls decrease as the extent of π-electron donation from the metal to the carbonyl ligands increase. The position of the carbonyl stretching frequencies of these complexes can be understood in terms of the ligand contribution to the stabilization of the electron deficient carbene carbon. Hence the structure **A** in figure 4.2 becomes more important.

The frequency of the vibration originating predominantly from the CO ligand *trans* to the carbene ligand of **10** and **11** occurs at a lower frequency (between 1923 and 1930 cm^{-1}) compared to that of the respective ethoxy carbene complexes. This is due to the lower π-accepting property of the carbene carbon in aminocarbene complexes which leads to the expansion of the t_{2g}-orbitals, thus making them available for interaction with the CO π*-orbitals.

Similar to the aminocarbene complexes **8** and **9**, the NH_2-group displayed two signals between 2850 and 2990 cm^{-1}.

4.4.1.4 Mass spectrometry

The M^+ signal was not observed in the mass spectra of the two bisaminocarbene complexes (**10** and **11**), and very few meaningful fragment ions displaying the transition metal isotope pattern could be observed.

4.5 Ultraviolet spectroscopy of the amino carbene complexes

Similar to ethoxy carbene complexes, aminocarbene complexes show a remarkable variation in colour. They absorb broad bands of visible radiation in at least one of their oxidation states by transition between filled and unfilled d-orbitals of the metal. The UV-spectra of these complexes were recorded in dichloromethane since they were insoluble in hexane. The electronic data of the aminocarbene compexes **8-11** are summarized in table 4.6.

Table 4.6 UV data[a] of complexes 8-11

Complex	Colour	Ligand π-π* - transitions	Metal-Ligand transitions	Ligand based absorptions
8	Pale yellow	409.0	460.0	265.0
9	Pale yellow	400.0	457.0	262.0
10	Orange	410.0	481.0	265.0
11	Orange	412.0	478.0	259.0

[a]UV peaks reported in nanometers (nm)

Only the ligand based absorptions and the metal-ligand transition peaks are clearly observed from the spectra. All the complexes exhibit a strong ligand based absorption band between 220 and 320 nm. The electronic spectrum of **9** is represented by figure 4.10 and that of complex **10** by figure 4.11. Intense absorptions around 360 nm are assigned to the terthienyl π-π*-transitions. Metal-ligand transition peaks of complex **8** and **9** underwent less bathochromic shift compared to their counterpart in ethoxy carbene complexes. This might have resulted from the stronger stabilization effect of the metal by the amino group, hence lessening the transitions in between. From these, one can say that for transition to take place effectively, the stabilization group must not be a strong electron releasing group.

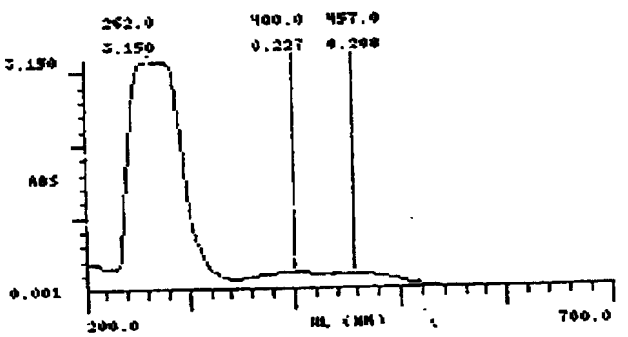

Figure 4.10 UV spectrum of 9

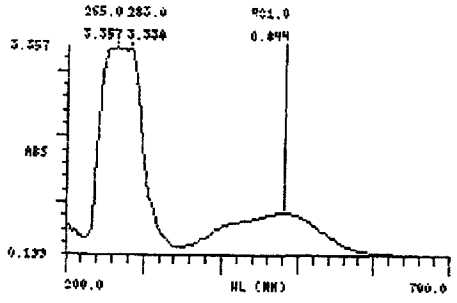

Figure 4.11 UV spectrum of 10

4.6 Conclusion

The objective was to study the aminolysis reaction of biscarbene complexes and compare the features of the products with those of the ethoxyterthienyl carbene complexes. Ammonia reacts immediately with the alkoxy carbene complexes to give aminocarbene complexes. Yellow products were obtained for monoaminocarbene complexes and orange-red rubbery products for bisaminocarbene complexes. These complexes are poorly soluble and little spectroscopic data could be obtained. Ultraviolet spectroscopy data also revealed the possibility of metal-metal communication in bisaminocarbenes complexes even though it was not so pronounced compared to in bisethoxycarbene complexes.

CHAPTER 5

CONCLUSION

Thiophene and its derivatives have proven to be very flexible substrates that are capable of adapting to the formation of complexes with different metal fragments. Efficient syntheses of these complexes are now available so it is important to investigate more closely the reactivity of these complexes and to apply in organic synthesis.

A marked increase in the stability was observed for biscarbene complexes of terthienyl compared to those thienothiophene and thiophene. The monocarbene complexes were stable for prolonged periods at room temperature in air. No kinetic studies were conducted on the biscarbene complexes and conclusions drawn were based on the stability of the complexes against decomposition in solution under inert atmosphere.

Biscarbene

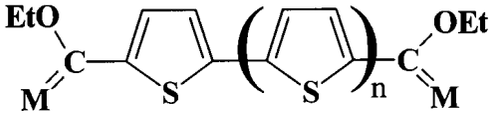

Stability (n): 0 < 1 < 2

Monocarbene

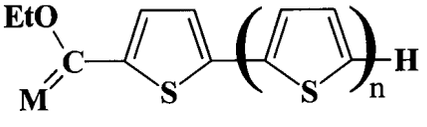

The longer the chain (n from 0 to 2) and the greater the conjugation possibilities of the spacer ligand, the stabler is the compound. Delocalization over three rings in biscabene complexes was not proved in the solid state, but bond-lengths revealed some delocalization in the first terthienyl ring, but extensive studies about π-delocalization capability of biscarbene complexes still need to be studied using other methods.

From comparison of the IR and NMR spectra of the symmetrically substituted terthienyl bridged complexes **10** and **11** with those of **7** and **8**, it follows that in the ground state there is only weak π-interaction between the thienyl, the $M(CO)_5$ and NH_2 fragments for bisaminocarbene complexes and $M(CO)_5$ and OEt fragments for bisethoxycarbene complexes through the spacer bridge.

Terthienyl biscarbene complexes could be very interesting to study with respect to charge conduction in molecular wires.

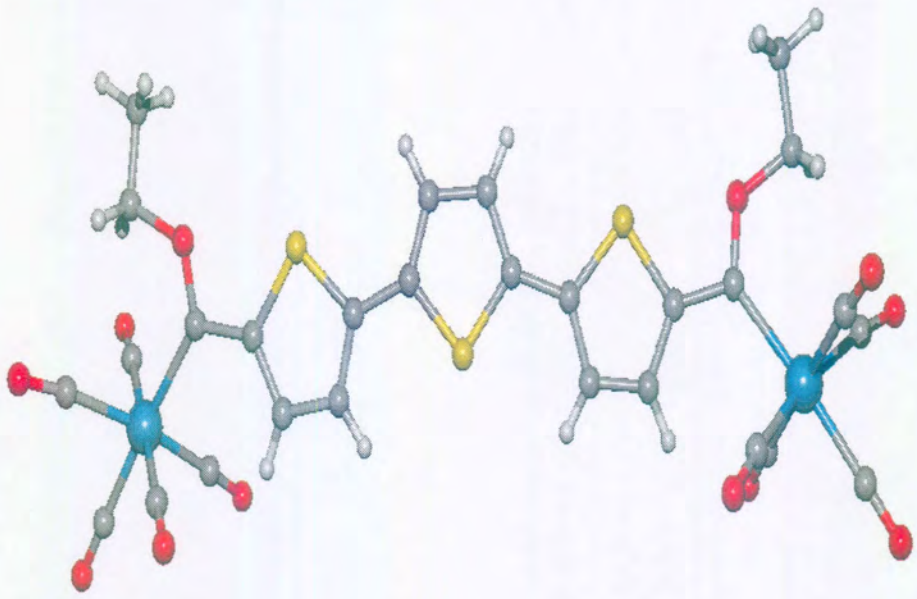

Figure 5.1 Crystal structure of complex 7

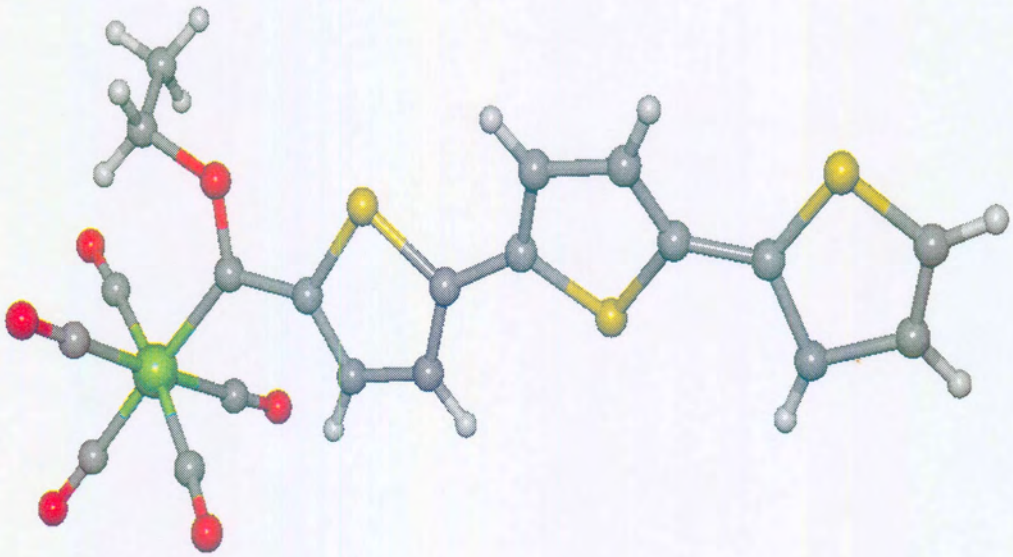

Figure 5.2 Crystal structure of complex 2

CHAPTER 6

EXPERIMENTAL SECTION

6.1. General details

Reagent grade tetrahydrofuran, diethylether, hexane and dichloromethane were dried and in addition, distilled before use. Tetrahydrofuran was dried and refluxed from sodium benzophenone ketyl. Ether was pre-dried from calcium chloride and refluxed from sodiumbenzophenone ketyl. Dichloromethane was dried and refluxed from diphosphorus pentoxide prior to use. Hexane was dried and refluxed from sodium metal.

The dilithiation method used is similar to that for dilithiation of thiophene[1]. Chromatography was performed on silica gel (0.063-0.200 mm) and the column (1.5 × 40 cm) cooled by recycling cold isopropanol (-40°C) through the column jacket. All the reaction manipulations were carried out under nitrogen atmosphere using schlenk tube techniques. Silica gel used for column chromatography was nitrogen saturated.

FTIR spectra were recorded on a Bomem Michelson-FT spectrophotometer using dichloromethane or hexane as solvents. Ten scans were recorded for each analysis. NMR experiments were performed on a multinuclear Bruker AC-300 spectrometer at low temperature (-20°C). Chemical shifts are given in ppm relative to the deuterium signal of the deuterated solvent for proton NMR spectra. The ^{1}H and ^{13}C-NMR spectra were measured at 300.15 and 75.469 MHz, respectively. Solvents used were deuterated chloroform, deuterated dichloromethane or deuterated acetone. UV spectra were recorded with the Genesis spectronic 5 spectrophotometer using dichloromethane as solvent. Mass spectra were recorded on a Perkin-Elmer RMU-6H instrument operating at 70eV. Melting points were recorded from a hot stage Gallenkamp melting point apparatus. X-ray crystal structure analysis were done from data collected at -90°C on a Nonius-Kappa CCD diffractometer using graphite-monochromated, Mo-Kα radiation. Data were corrected for Lorenz polarization effects. Structures were solved by direct methods (SHELXS) and refined by full-matrix least squares techniques.

---

[1] L.Brandsma, S.F.Vasilevsky, H.D.Verkruijsse, Application of Transition Metal Catalysts in Organic Synthesis, ISBN 3-540-62831-2 Springer-Verlag Berlin Heidelberg New York.

5.2. SYNTHESIS OF TERTHIENYL

Synthesis of terthienyl involved three steps. The first step was the synthesis of 3-dimethylamino-1-(2-thienyl)-propanone HCl (DTPH) , followed by the synthesis of 1,4-di-(2-thienyl)-1,4-butanedione (DTB) and finally the synthesis of α-terthienyl (HTTTH).

Step 1 Synthesis of DTPH

A mixture of 63 g (0.5 mole) of 2-acetylthiophene (2-AT), 18 g (0.6 mole) paraformaldehyde, 49 g (0.6 mole) dimethylamino.HCl (DAH) and 2.5 ml concentrated HCl in 60 ml of 95% ethyl alcohol was heated under reflux for 16 hours. Cooling produced 91 g (83%) of the product Mannich base hydrochloride (MbH). 2.5 g of the MbH was made alkaline (in water) using ammonia solution and extracted three times using ether. Washing and drying of the ether layer, followed by evaporation of the solvent afforded 1.85 g of Mannich base (Mb). The Mb was used at once in the second step.

Step 2 Synthesis of DTB

A solution of freshly distilled 2-thiophene aldehyde (2-TA) (1.4 g, 12.5 mmol) in 4 ml dry DMF under a nitrogen atmosphere was added over a period of 15 minutes to a suspension of 0.31 g (6.3 mmol) NaCN in 4 ml dry DMF. After the mixture had been stirred for 15 minutes, the free Mb (1.83 g, 10 mmol) in 10 ml dry DMF was added over a period of one hour. The solution was allowed to stand overnight. The overnight solution turned yellowish-green in colour. Water was added and the solution was extracted three times with chloroform. The chloroform layer was washed and dried from $MgSO_4$. Chloroform was then removed under vacuum and recrystalized from ethanol and shiny white crystals of DTB (1.75 g, 70%) with melting point of 131-133°C (lit. 130-131°C)[2] were obtained.

[2] H.J.Kooreman, H.Wynberg, Rec.Trav.Chim., 1967, 86, 37.

Step 3 Synthesis of HTTTH

To a solution of 0.250 g (1 mmol) of diketone (DTB) in 5 ml of ether, 1.11 g (2.5 mmol) P_2S_5 was added with stirring. Sodium bicarbonate was added at such a rate that smooth CO_2 evolution occurred[3]. The solution was decomposed with water and then extracted three times with ether. The solution was dried and the solvent removed under vacuum. The crystals were purified with column chromatography and recystallized with ethanol. HTTTH (0.180 g, 70%) with a melting point of 94-95°C was afforded.

6.3. SYNTHESIS OF CARBENE COMPLEXES

All the carbene complexes decomposed before melting points could be observed.

6.3.1 Preparation of $[(CO)_5WC(OEt)C_{12}H_6S_3C(OEt)W(CO)_5]$ 7 and $[W(CO)_5C(OEt)C_{12}H_7S_3]$ 4

3,05 ml (4.80 mmol) of n-BuLi was added to a solution of 0,67 g (4.44 mmol) of tetramethylethylenediamine (TMEDA) and 0.550 g (2.21 mmol) α-Terthienyl in 30 ml hexane at room temperature (rt.). A yellowish suspension gradually formed and refluxing for 30 minutes completed the conversion (dilithiation of α-terthienyl substrate). The suspension was cooled to below 0°C and 40 ml freshly distilled THF was added. After further cooling to –40°C, 1.72 g (4.88 mmol) of $W(CO)_6$ was gradually added to the vigorously stirred mixture. The reaction mixture turned dark brown in colour. The temperature was then allowed to rise to room temperature and stirring was maintained for a further 20 minutes during which time the colour changed to reddish–brown. After the reaction had been completed, all solvents were removed under reduced pressure and a dry brown solid was obtained. 0.95 g (4.88 mmoles) of triethyloxonium tetrafluoroborate, dissolved in 30 ml of dichloromethane, was carefully added to the stirred brown mixture at –30°C and the mixture turned purple. The purple reaction

[3] J.W.Scheeren, P.H.J.Oomes, R.J.F.Nivard, Synthesis, 1973, 149.

mixture was washed through a filter containing anhydrous sodium sulphate and silica gel with dichloromethane. Volatile materials were removed under reduced pressure. The residue was dissolved in 50 ml of dichloromethane, adsorbed onto silica gel and dried *in vacuo*. The resulting solid material was placed on a pre-packed column. The product was purified starting with hexane as eluting agent, and gradually increasing the polarity by adding dichloromethane until the product could be isolated using hexane and dichloromethane (*1:1*). Three bands separated. The first yellow band isolated yielded the butyl carbene complex, $[Cr\{C(OEt)Bu\}(CO)_5]$[4]. The second brownish band afforded 0.295 g (21.5%) of the mononuclear terthienyl carbene complex **4** and the third purple zone afforded 1.350 g (60.5%) of the dinuclear terthienylbiscarbene complex **7**.

6.3.2. Preparation of $[(CO)_5CrC(OEt)C_{12}H_6S_3C(OEt)Cr(CO)_5]$ 5 and $[Cr(CO)_5C(OEt)C_{12}H_7S_3]$ 2

These complexes were prepared in the same way as **4** and **7**. From 0.590 g of α-terthienyl (2.38 mmol), 1.150 g of the dinuclear terthienyl biscarbene complex **5** (65%) and 0.206 g of the mononuclear terthienyl carbene cmplex **2** (20%) were afforded.

6.3.3. Preparation of $[(CO)_5MoC(OEt)C_{12}H_6S_3C(OEt)Mo(CO)_5]$ 3 and $[Mo(CO)_5C(OEt)C_{12}H_7S_3]$ 6

These complexes were prepared in the same way as **4** and **7**. From 0.420 g of α-terthienyl (1.69 mmol), 0.881 g of the dinuclear biscarbene complex **6** (63%) and 0.163 g of the mononuclear terthienyl carbene complex **3** (18%) were afforded.

6.4. AMINOLYSIS OF THE CARBENE COMPLEXES

6.4.1. Preparation of $[(CO)_5WC(NH_2)C_{12}H_6S_3C(NH_2)W(CO)_5]$ 11

[4] M.Y.Darensbourg, D.J.Darensbourg, Inorg.Chem.,1970, 9, 32.

Gaseous ammonia was bubbled through a solution of 0.88 g (0.87 mmol) of **7** in 50 ml ether. The initial deep purple solution rapidly became light orange. The solvent was evaporated off under reduced pressure. The residue was dissolved in ether, adsorbed onto silica gel and dried *in vacuo*. The resulting solid material was placed on a prepacked column. The product was purified by starting with hexane as eluting agent, and gradually increasing the polarity by adding ether until the product could be isolated using a mixture of hexane and ether (1:1) .

Two bands were collected and separated. The second light orange zone was isolated after a grey band (less than 5 %) eluted which was discarded. The orange zone afforded 0.657 g (79%) of **11**. The product was recrystallized from the mixture of hexane:ether (9:1).

6.4.2. Preparation of $[W(CO)_5C(NH_2)C_{12}H_7S_3]$ 9

This complex was prepared in the same way as **11**. From 50 mg of **4** (0.0797 mmol) in 50 ml ether, 39.7 mg of **9** was isolated. The afforded yield is 83.3% and again no melting point could be recorded as the compound decomposed on heating. In the solvent the product **9** was yellow in colour, but after the removal of the solvent under reduced pressure at very low temperature, light brown crystals of **9** were obtained.

6.4.3. Preparation of $[(CO)_5CrC(NH_2)C_{12}H_6S_3C(NH_2)Cr(CO)_5]$ 10

This complex was prepared in the same way as **11**. From 400 mg of **5** (0.270 mmol) in 100 ml ether, 0.328 g of **10** was isolated and 89% yield was obtained.

6.4.4. Preparation of $[(CO)_5CrC(NH_2)C_{12}H_7S_3]$ 8

Compound **8** was prepared by the same method as **11** starting with 0.200 g of **2** (0.40 mmol). An orange product **8** (0.162 g, 86%) was obtained.

APPENDIX

Table 1: Crystal data and structure refinement for complex 7

Empirical formula	$C_{28}\ H_{16}\ O_{12}\ S_3\ W_2$	
Formula weight	1008.29	
Temperature	183(2) K	
Wavelength	0.71073 Å	
Crystal system	Monoclinic	
Space group	C2/c	
Unit cell dimensions	a = 16.2331(7) Å	α= 90°.
	b = 17.4483(9) Å	β= 106.187(3)°.
	c = 12.1952(6) Å	γ = 90°.
Volume	3317.2(3) $Å^3$	
Z	4	
Density (calculated)	2.019 Mg/m^3	
Absorption coefficient	7.177 mm^{-1}	
F(000)	1904	
Crystal size	0.22 x 0.12 x 0.06 mm^3	
Theta range for data collection	3.48 to 27.51°.	
Index ranges	$-20 \le h \le 19, -20 \le k \le 22, -15 \le l \le 14$	
Reflections collected	12623	
Independent reflections	3743 [R(int) = 0.0508]	
Completeness to theta = 27.51°	98.2 %	
Absorption correction	Semi-empirical	
Max. and min. transmission	0.418 and 0.274	
Refinement method	Full-matrix least-squares on F^2	
Data / restraints / parameters	3743 / 0 / 204	
Goodness-of-fit on F^2	1.018	
Final R indices [I>2sigma(I)]	R1 = 0.0343, wR2 = 0.0597	
R indices (all data)	R1 = 0.0537, wR2 = 0.0641	
Largest diff. peak and hole	0.676 and -1.100 $e.Å^{-3}$	

Table 2: Atomic coordinates (x 10^4) and equivalent isotropic displacement parameters ($Å^2$x 10^3) for 7. U (eq) is defined as one third of the trace of the orthogonalized U^{ij} tensor.

	x	y	z	U(eq)
W(1)	8463(1)	1323(1)	3716(1)	28(1)
S(1)	6515(1)	-186(1)	683(1)	29(1)
S(2)	5000	867(1)	-2500	33(1)
O(1)	7549(2)	-318(2)	2906(2)	30(1)
O(2)	8787(3)	2104(2)	1517(3)	59(1)
O(3)	6772(3)	2282(2)	3646(3)	57(1)
O(4)	9621(3)	2679(3)	5036(4)	88(2)
O(5)	8561(2)	789(2)	6258(3)	45(1)
O(6)	10190(2)	413(3)	3857(3)	61(1)
C(1)	7608(3)	432(3)	2688(4)	26(1)
C(2)	7002(3)	573(2)	1581(4)	27(1)
C(3)	6734(3)	1271(3)	1047(4)	33(1)
C(4)	6162(3)	1193(3)	-50(4)	34(1)
C(5)	5989(3)	435(3)	-388(4)	27(1)
C(6)	5460(3)	179(3)	-1497(4)	28(1)
C(7)	5267(3)	-544(3)	-1931(4)	34(1)
C(8)	8118(3)	-678(3)	3915(4)	38(1)
C(9)	8057(4)	-1520(3)	3720(5)	53(2)
C(10)	8630(3)	1809(3)	2279(4)	38(1)
C(11)	7377(3)	1940(3)	3667(4)	37(1)
C(12)	9207(4)	2187(4)	4569(5)	50(2)
C(13)	8486(3)	939(3)	5326(4)	35(1)
C(14)	9557(3)	715(3)	3800(4)	37(1)

Table 3: Bond lengths [Å] and angles [°] for 7.

W(1)-C(12)	2.027(6)
W(1)-C(10)	2.032(5)
W(1)-C(14)	2.047(5)
W(1)-C(11)	2.053(5)
W(1)-C(13)	2.066(5)
W(1)-C(1)	2.225(5)
S(1)-C(5)	1.728(4)
S(1)-C(2)	1.760(4)
S(2)-C(6)#1	1.727(4)
S(2)-C(6)	1.727(4)
O(1)-C(1)	1.344(5)
O(1)-C(8)	1.459(5)
O(2)-C(10)	1.151(6)
O(3)-C(11)	1.143(6)
O(4)-C(12)	1.140(6)
O(5)-C(13)	1.139(6)
O(6)-C(14)	1.139(6)
C(1)-C(2)	1.453(6)
C(2)-C(3)	1.393(6)
C(3)-C(4)	1.406(6)
C(4)-C(5)	1.391(6)
C(5)-C(6)	1.455(6)
C(6)-C(7)	1.371(6)
C(7)-C(7)#1	1.417(9)
C(8)-C(9)	1.488(7)
C(12)-W(1)-C(10)	85.9(2)
C(12)-W(1)-C(14)	88.6(2)
C(10)-W(1)-C(14)	86.39(18)
C(12)-W(1)-C(11)	90.5(2)
C(10)-W(1)-C(11)	94.38(18)

C(14)-W(1)-C(11)	178.82(19)
C(12)-W(1)-C(13)	84.5(2)
C(10)-W(1)-C(13)	169.78(19)
C(14)-W(1)-C(13)	89.93(18)
C(11)-W(1)-C(13)	89.16(19)
C(12)-W(1)-C(1)	176.1(2)
C(10)-W(1)-C(1)	91.03(18)
C(14)-W(1)-C(1)	93.56(18)
C(11)-W(1)-C(1)	87.33(17)
C(13)-W(1)-C(1)	98.72(17)
C(5)-S(1)-C(2)	92.3(2)
C(6)#1-S(2)-C(6)	92.1(3)
C(1)-O(1)-C(8)	121.5(3)
O(1)-C(1)-C(2)	106.4(4)
O(1)-C(1)-W(1)	129.6(3)
C(2)-C(1)-W(1)	124.1(3)
C(3)-C(2)-C(1)	128.7(4)
C(3)-C(2)-S(1)	109.9(3)
C(1)-C(2)-S(1)	121.4(3)
C(2)-C(3)-C(4)	113.4(4)
C(5)-C(4)-C(3)	113.6(4)
C(4)-C(5)-C(6)	125.8(4)
C(4)-C(5)-S(1)	110.9(3)
C(6)-C(5)-S(1)	123.3(3)
C(7)-C(6)-C(5)	130.8(4)
C(7)-C(6)-S(2)	111.0(4)
C(5)-C(6)-S(2)	118.2(3)
C(6)-C(7)-C(7)#1	112.9(3)
O(1)-C(8)-C(9)	107.0(4)
O(2)-C(10)-W(1)	174.6(5)
O(3)-C(11)-W(1)	179.7(5)
O(4)-C(12)-W(1)	179.0(6)
O(5)-C(13)-W(1)	172.5(4)

O(6)-C(14)-W(1)	176.2(5)

Symmetry transformations used to generate equivalent atoms:
#1 -x+1,y,-z-1/2

Table 4: Anisotropic displacement parameters ($Å^2 x\ 10^3$) for 7. The anisotropic displacement factor exponent takes the form: $-2\pi^2 [h^2 a^{*2} U^{11} + ... + 2 h k a^* b^* U^{12}]$

	U^{11}	U^{22}	U^{33}	U^{23}	U^{13}	U^{12}
W(1)	32(1)	29(1)	23(1)	-4(1)	8(1)	-5(1)
S(1)	30(1)	28(1)	25(1)	0(1)	1(1)	0(1)
S(2)	37(1)	31(1)	25(1)	0	-1(1)	0
O(1)	35(2)	27(2)	24(2)	1(1)	0(1)	-2(1)
O(2)	80(3)	57(3)	47(2)	14(2)	30(2)	0(2)
O(3)	64(3)	55(3)	55(3)	-4(2)	22(2)	24(2)
O(4)	97(4)	81(4)	98(4)	-50(3)	49(3)	-63(3)
O(5)	50(2)	60(3)	26(2)	1(2)	13(2)	-2(2)
O(6)	43(2)	90(3)	52(3)	18(2)	16(2)	21(2)
C(1)	24(2)	32(3)	24(2)	1(2)	11(2)	7(2)
C(2)	26(2)	26(2)	27(2)	-1(2)	6(2)	4(2)
C(3)	41(3)	31(3)	24(2)	-3(2)	5(2)	5(2)
C(4)	35(3)	28(3)	33(3)	-1(2)	1(2)	11(2)
C(5)	24(2)	35(3)	23(2)	3(2)	7(2)	6(2)
C(6)	27(2)	30(3)	25(2)	2(2)	3(2)	4(2)
C(7)	28(2)	36(3)	35(3)	2(2)	4(2)	4(2)
C(8)	46(3)	35(3)	25(3)	4(2)	0(2)	0(2)
C(9)	85(4)	29(3)	41(3)	8(2)	12(3)	7(3)
C(10)	41(3)	33(3)	42(3)	-1(2)	14(3)	7(2)

C(11)	52(3)	29(3)	33(3)	-4(2)	15(2)	-1(2)
C(12)	50(3)	60(4)	48(3)	-14(3)	27(3)	-20(3)
C(13)	28(2)	39(3)	40(3)	-7(2)	11(2)	-6(2)
C(14)	37(3)	50(3)	25(3)	4(2)	7(2)	-2(2)

Table 5: Hydrogen coordinates (x 10^4) and isotropic displacement parameters ($Å^2$x 10^3) for 7.

	x	y	z	U(eq)
H(3A)	6919	1753	1390	40
H(4A)	5918	1617	-516	40
H(7A)	5471	-998	-1513	41
H(8A)	7939	-544	4604	45
H(8B)	8715	-502	4026	45
H(9A)	8434	-1784	4380	79
H(9B)	8232	-1645	3034	79
H(9C)	7463	-1687	3617	79